TECHNICAL REPORT BRL-TR-29 0

AD-A195 666

BRL

1938 – Serving the Army for Fifty Years – 1988

PARAMETERS FOR OPTIMIZING A TRAVELING CHARGE GUN SYSTEM

WILLIAM F. OBERLE
GLORIA P. WREN
FRED W. ROBBINS
KEVIN J. WHITE
ROBERT E. TOMPKINS
ARPAD A. JUHASZ

DTIC
ELECTE
JUL 22 1988
S D
D

MAY 1988

APPROVED FOR PUBLIC RELEASE; DISTRIBUTION UNLIMITED.

U.S. ARMY LABORATORY COMMAND

BALLISTIC RESEARCH LABORATORY

ABERDEEN PROVING GROUND, MARYLAND

UNCLASSIFIED

SECURITY CLASSIFICATION OF THIS PAGE

REPORT DOCUMENTATION PAGE

Form Approved OMB No. 0704-0188

1a. REPORT SECURITY CLASSIFICATION Unclassified	1b. RESTRICTIVE MARKINGS
2a. SECURITY CLASSIFICATION AUTHORITY	3. DISTRIBUTION/AVAILABILITY OF REPORT
2b. DECLASSIFICATION/DOWNGRADING SCHEDULE	
4. PERFORMING ORGANIZATION REPORT NUMBER(S) BRL-TR-2910	5. MONITORING ORGANIZATION REPORT NUMBER(S)
6a. NAME OF PERFORMING ORGANIZATION US Army Ballistic Rsch Lab 6b. OFFICE SYMBOL (If applicable) SLCBR-IB-B	7a. NAME OF MONITORING ORGANIZATION
6c. ADDRESS (City, State, and ZIP Code) Aberdeen Proving Ground, MD 21005-5066	7b. ADDRESS (City, State, and ZIP Code)
8a. NAME OF FUNDING/SPONSORING ORGANIZATION 8b. OFFICE SYMBOL (If applicable)	9. PROCUREMENT INSTRUMENT IDENTIFICATION NUMBER
8c. ADDRESS (City, State, and ZIP Code)	10. SOURCE OF FUNDING NUMBERS PROGRAM ELEMENT NO. / PROJECT NO. / TASK NO. / WORK UNIT ACCESSION NO.

11. TITLE (Include Security Classification)
PARAMETERS FOR OPTIMIZING A TRAVELING CHARGE GUN SYSTEM

12. PERSONAL AUTHOR(S)
Oberle, W.F., Wren, G.P., Robbins, F.W., White, K.J., Tompkins, R.E., and Juhasz, A.A.

13a. TYPE OF REPORT	13b. TIME COVERED	14. DATE OF REPORT (Year, Month, Day)	15. PAGE COUNT
TR	FROM _____ TO _____		

16. SUPPLEMENTARY NOTATION

17. COSATI CODES			18. SUBJECT TERMS (Continue on reverse if necessary and identify by block number)
FIELD	GROUP	SUB-GROUP	cont'd p 1

19. ABSTRACT (Continue on reverse if necessary and identify by block number)

Previous work at the Ballistic Research Laboratory has demonstrated that the XNOVAKTC computer code is a reliable tool for the simulation of traveling charge gun firings when compared to experimental results. Thus, it was felt that the code could be utilized to address many realistic questions associated with the traveling charge concept. An important question of primary interest is how to tailor both the booster and traveling charge to obtain optimized ballistic performance. Therefore, the purpose of this study is to provides guidelines for optimization of traveling charge gun systems and to assess the applicability of these guidelines to a 14-mm (gun) test fixture.

In the study, the XNOVAKTC computer code is used to investigate parameters which significantly impact performance. The base study is performed on a hypothetical 14-mm gun

20. DISTRIBUTION/AVAILABILITY OF ABSTRACT ☐ UNCLASSIFIED/UNLIMITED ☒ SAME AS RPT. ☐ DTIC USERS	21. ABSTRACT SECURITY CLASSIFICATION Unclassified
22a. NAME OF RESPONSIBLE INDIVIDUAL William F. Oberle	22b. TELEPHONE (Include Area Code) (301) 278-6200 22c. OFFICE SYMBOL SLCBR-IB-B

DD Form 1473, JUN 86 Previous editions are obsolete.

SECURITY CLASSIFICATION OF THIS PAGE

UNCLASSIFIED

19. ABSTRACT (Con't)

with pressure and propellant constraints attainable in this system. A general set of guidelines is developed for optimal performance in the 14-mm gun. ~~The results~~ of this ~~study are then~~ applied to the 14-mm test fixture at BRL.

The results of the study indicate that the traveling charge effect is real and demonstrable, yielding increased velocities at lower chamber pressures. The greatest payoff seems to be for systems with high propellant mass to projectile mass ratios, i.e. high projectile velocity applications. If the obstacle in timing TC ignition and burnout can be overcome, potential velocity improvements of up to 30% ~~percent~~ appear possible.

TABLE OF CONTENTS

		Page
	LIST OF FIGURES	v
	LIST OF TABLES	vii
I.	INTRODUCTION	1
II.	NUMERICAL MESH INDIFFERENCE AND COMPUTER CODE VALIDATION	3
	1. NUMERICAL MESH INDIFFERENCE	4
	2. COMPUTER CODE VALIDATION	5
III.	PARAMETRIC INVESTIGATIONS	14
	1. CHAMBER GEOMETRY STUDY	14
	2. TC IGNITION TIME/LOCATION OF TC BURNOUT	17
	3. TC PROPELLANT BURN RATE	22
	4. BOOSTER PROPELLANT GEOMETRY	23
	5. CHARGE-TO-MASS RATIO FOR 14-MM TEST FIXTURE	25
IV.	OPTIMAL PERFORMANCE FOR 14-MM BRL TEST FIXTURE	28
V.	CONCLUSIONS	30
	REFERENCES	31
	DISTRIBUTION LIST	33

DTIC COPY INSPECTED 6

Accesion For
NTIS CRA&I ☑
DTIC TAB ☐
Unannounced ☐
Justification
By
Distribution /
Availability Codes
Dist | Avail and / or Special
A-1

LIST OF FIGURES

Figure		Page
1	Idealized Traveling Charge Combustion	2
2	Schematic of Experimental Gun Fixture (dimensions in cm)	4
3a	Computed Pressure-Time Profiles for a Conventional Gun Firing	6
3b	Experimental Pressure-Time Profiles for a Conventional Gun Firing	7
4a	Computed P/T Profiles for a Traveling Charge Gun Firing	9
4b	Experimental P/T Profiles for a Traveling Charge Fun Firing	9
5	Comparison of Velocity for Computed and Experimental Results	10
6	ID 44, Experimental Pressure	11
7	Experimental Velocity	12
8	Simulation of ID 44 Pressure	13
9	Simulation of ID 44 Velocity	13
10	Varying Diameter for Differing Amounts of Chambrage	15
11	Discontinuity Resulting From Having No Taper Length	16
12	Velocity Versus Chamber Length	17
13	Velocity Versus TC Ignition Time for a Variety of Simulations	19
14	Velocity Versus Location of TC Burnout	21
15	Base Pressure Versus Travel for Conventional and Traveling Charge Simulations	21
16	Percent Change in Velocity Versus Percent Change in the Burn Rate Coefficient Describing the TC Combustion	23

LIST OF FIGURES (CON'T)

Figure		Page
17	Comparison Between Conventional and Traveling Charge Velocities for Various Charge-to-Mass Ratios	27

LIST OF TABLES

Table		Page
1	XKTC Results for Different Number of Mesh Points -- Traveling Charge Mode of Operation	4
2	Comparison of Predicted XKTC Results and Experimental Results for a Conventional Firing	5
3	Comparison of Predicted XKTC Results and Experimental Results for Traveling Charge Firing	8
4	Velocity (m/s) for Various Chamber and Taper Lengths	16
5	Velocity as a Function of TC Ignition Time	18
6	Velocity Results for Changing Burn Rate Coefficient Describing the TC Combustion	22
7	Optimization as a Conventional Gun System for Different Propellant Geometries, 26 g Projectile	24
8	Velocity Corresponding to Various Booster Propellant Geometries in TC Gun Systems	24
9	Optimal Velocity for Different Booster Propellant Geometries with the Maximum Amount of TC	25
10	Velocity for Varying Charge-to-Mass Ratios in Conventional and Traveling Charge Simulations	26
11	Percentage Increases in Velocity Resulting from Using TC Over Conventional for Various Charge-to-Mass Ratios	26
12	Energy Distribution from Conventional and Traveling Charge Calculations	28
13	XKTC Optimization of Experimental 14-mm Gun Fixture	29

I. INTRODUCTION

Originally proposed by Langweiler,[1] in the early 1940's, the traveling charge concept ~~(or "impulse gun")~~ is a solid propellant propulsion technique thought by ballisticians to offer the prospect of muzzle exit velocities in the 2 to 3 km/s range without the high breech pressures ~~(700-1000 MPa)~~ required of conventional gun propulsion systems. Resulting advantages of velocities of this magnitude have been discussed by various authors[1-3] and can be summarized as improved delivery range, increased target penetration due to higher kinetic energy of the projectile, and enhanced hit probability resulting from the decreased time-of-flight from muzzle to target.

An idealized description of the traveling charge effect has been presented in an earlier work by Smith[4] and is shown in Figure 1. The process is in two stages. Ignition of a conventional granular booster charge is used to rapidly pressurize the chamber and accelerate both the projectile and a very high burning rate (VHBR) traveling charge, (TC) attached to the base of the projectile. At some point during this initial pressurization, usually past the peak pressure due to the booster charge, the traveling charge is ignited. Subsequent idealized burning of the TC is tailored to eject combustion products at sufficient velocity so as to maintain constant thrust/pressure on the base of the projectile until burnout of the propellant is achieved. In a conventional gun, high velocities can be achieved by using more propellant. As the projectile leaves the gun, a considerable amount of the chemical energy has gone into accelerating the combustion gases. This causes a large pressure gradient between the chamber and the projectile. In the traveling charge concept the TC propellant is burning such that the gas velocities at muzzle exit are reduced compared with the conventional charge. Consequently, less chemical energy is used in accelerating the combustion gases. Thus at very high velocities, the traveling charge is expected to be more efficient than conventional propelling charges.

In summary, the idealized traveling charge effect is characterized by:

a) The attachment to the projectile of a very high burning rate propellant which travels with the projectile down the tube during the ballistic event.

b) Burning of the TC propellant in such a manner as to produce a constant thrust/pressure on the projectile base.

c) Deviation from the "normal" pressure gradient which would be obtained if all the propellant, booster and TC, were placed in the chamber. The deviation should show lower peak chamber pressures and increased downbore pressures.

d) An increase in muzzle velocity over the corresponding conventional firing where all the propellant is located in the chamber.

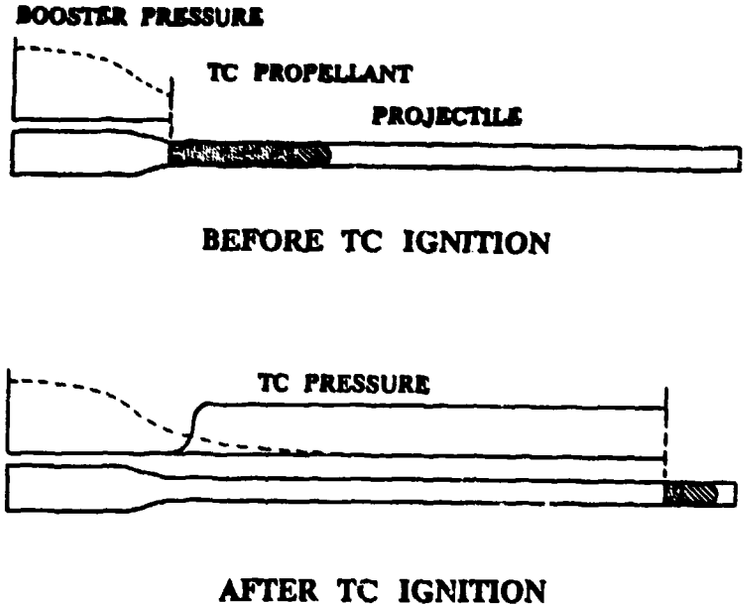

Figure 1. Idealized Traveling Charge Combustion[4]

Since achieving propellant burning to obtain the constant thrust/pressure on the projectile base required for the idealized TC scenario is not yet at hand, many realistic questions associated with the traveling charge concept need to be addressed. Of primary interest is the identification of parameters, of the gun system and of both the booster and traveling charge, which have an effect on performance and how they can be tailored to obtain optimized ballistic results. Thus, a series of parametric calculations, utilizing the computer code XNOVAKTC, was performed to determine the effect of several factors which were felt might impact traveling charge performance. The emphasis in all studies was to determine a set of realistic conditions which could be imposed on the gun system, a 14-mm test fixture. Therefore, idealized conditions such as ideal burning of the TC, constant pressure/thrust on projectile base, were not considered. The parameters studied were:

a) Gun chamber geometry

b) TC ignition time/location of TC burnout

c) TC propellant burn rate

d) Booster propellant geometry

e) Charge-to-mass ratio

In addition, the Ballistic Research Laboratory (BRL) is involved in an experimental effort to demonstrate the traveling charge concept as a practical and useful gun propulsion system in a 14-mm bore diameter test fixture. The results of the parametric studies were, therefore, applied to the BRL test fixture to determine potential optimal performance. Computer predictions were also correlated to experimental firings with results reported in a companion paper.[5]

The purpose of this report is to validate the use of the computer code XNOVAKTC, summarize findings of the parametric studies, and assess the applicability of these findings to the BRL traveling charge gun program.

II. NUMERICAL MESH INDIFFERENCE AND COMPUTER CODE VALIDATION

The computer code selected to model the interior ballistic event was the XNOVAKTC (XKTC) code developed by Paul Gough Associates. This code is a combination of a newer version of the NOVA[6] code together with the BRLTC[7] code. Selection of XKTC was based upon several factors. First, the code has the capability to model the interior ballistics of conventional and traveling charge guns as well as a combination of conventional propellant booster and traveling charge guns. Second, the code includes kinetic options which allow flexibility in investigating the traveling charge effect. The final factor in selecting XKTC was its demonstrated accuracy in predicting gun performance, in terms of pressure profiles, pressure oscillations, and velocity.

In an earlier report,[8] XKTC'S predictive ability for small caliber systems was demonstrated. In this report we summarize the earlier results and address the down-bore pressure discrepancies reported in the earlier work. Exact details of the experimental setup, which was used to provide initial input to XKTC, will not be presented in this report but can be found in the companion paper.[5] However, for reference purposes, a schematic of the gun fixture showing pressure port locations is shown in Figure 2. The fixture is a 14-mm Mann barrel with a total length of 290 cm.

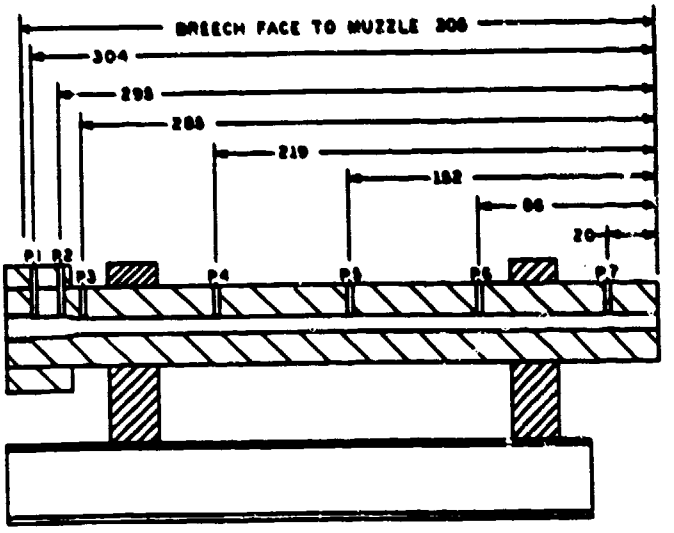

Figure 2. Schematic of Experimental Gun Fixture (dimensions in cm)

1. NUMERICAL MESH INDIFFERENCE

To determine the numerical dependence of XKTC as a function of the number of mesh points used in the computation the code was run using the traveling charge option. As mentioned above, the input parameters used in the code modeled the 14-mm experimental fixture in terms of gun geometry, projectile mass, and propellant combustion characteristics. For this study 40 g of booster propellant (non-deterred, unrolled small arms, ball, Olin X-4179) and 8 g of traveling charge (same thermochemistry as booster) were used in the calculations. Results from XKTC for various number of mesh points are presented in Table 1.

TABLE 1. XKTC Results for Different Number of Mesh Points -- Traveling Charge Mode of Operation

Number of Mesh Pts. (-)	Max Breech Pressure (MPa)	Time to Max Breech Pressure (ms)	Muzzle Exit Velocity (m/s)	Final Energy Defect (-)	Final Mass Defect (-)
15	437.3	1.217	2303.7	-12.85%	-14.27%
31	434.0	1.228	2304.3	+3.11%	+4.84%
41	434.4	1.216	2306.7	+0.82%	+1.87%
51	434.8	1.227	2307.8	-2.04%	-2.43%
61	434.8	1.226	2308.3	+0.77%	+1.57%

As can be seen from Table 1, the maximum breech pressure and muzzle exit velocity are almost identical for the different number of mesh points used. However, for 15 mesh points large energy and mass defects are obtained. Using 31 or more mesh points reduces energy and mass defects with the best results obtained for 41 or 61 mesh points. Based upon those results, it appears that given a reasonable number of mesh points XKTC calculations for this system are mesh independent. For the studies performed the mesh size was chosen to be 41.

2. COMPUTER CODE VALIDATION

To determine XKTC's capability to simulate small caliber gun firings and to validate the code, comparisons were made between experimental gun firing results and computer simulations for both a conventional and a traveling charge gun firing.

To match the experimental conventional gun firing, the XKTC code was run in a conventional gun firing mode. Burn rates for the propellant were obtained through closed chamber experiments. The mass of propellant, which was a non-deterred ball (used to avoid burn rate uncertainties associated with deterred propellant), was 34 g, and the projectile mass was 24.6 g. Table 2 shows the final computed results after a series of parametric runs which involved varying the shot start pressure and bore resistance profile. The final row of data in the table presents the difference between computed and experimentally measured pressures and velocities. Overall, the agreement between experiment and computation was excellent, except for gage 5. Computed pressure-time (P/T) profiles from XKTC together with experimental P/T profiles are presented in Figure 3. A comparison of the computed and experimental maximum pressure shows the excellent agreement for maximum breech pressure as indicated in Table 2. Differences in the maximum downbore pressures range from -8.5% to 4% In addition, the timing of the events (uncovering of gage locations, etc.) are in close agreement, which supports the velocity agreement of 0.1%.

TABLE 2. Comparison of Predicted XKTC Results and Experimental Results for a Conventional Firing

Gage 1 Pmax (MPa)	Gage 2 Pmax (MPa)	Gage 3 Pmax (MPa)	Gage 5 Pmax (MPa)	Gage 7 Pmax (MPa)	Velocity Interferometer (m/s)
XKTC -- Computed					
341	338	275	65	28	1571
Experimental -- Conventional Firing (ID 6):					
340	325	281	71	28	1570
Difference:					
1	13	-6	-6	0	1

TABLE 2. Comparison of Predicted XKTC Results and Experimental Results for a Conventional Firing (Con't)

Gage 1 Pmax (MPa)	Gage 2 Pmax (MPa)	Gage 3 Pmax (MPa)	Gage 5 Pmax (MPa)	Gage 7 Pmax (MPa)	Velocity Interferometer (m/s)
Percent Difference:					
.3%	4%	-2%	-8.5%	0%	0.1%

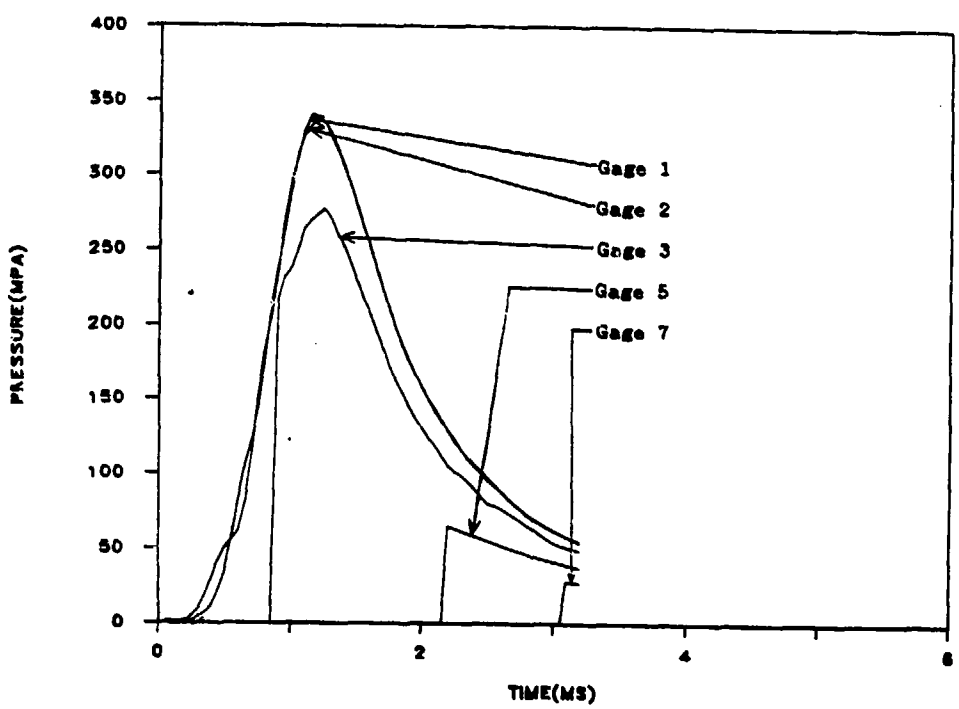

Figure 3a. Computed Pressure-Time Profiles for a Conventional Gun Firing

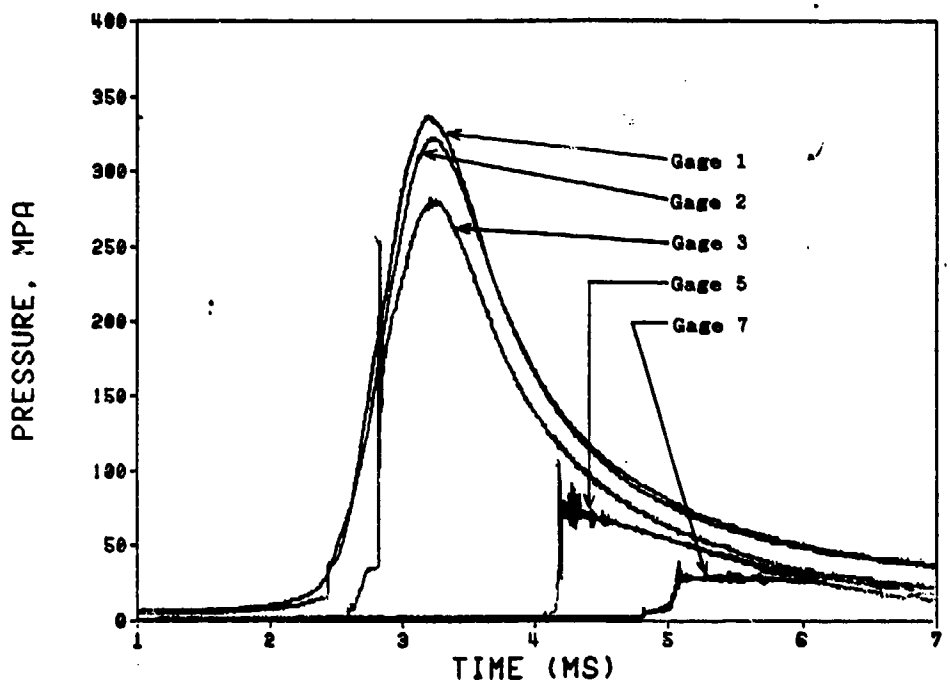

Figure 3b. Experimental Pressure-Time Profiles for a Conventional Gun Firing

Based upon the success in matching experimental results for the conventional gun firing, all input variables, except those pertaining specifically to the traveling charge and booster charge weights, were fixed in trying to match the results of the experimental traveling charge gun firings. A burning rate law ($r=bP^n$, where b=30.7 cm/(sec-MPa) and n=1.05) was used to describe the traveling charge burning. The values used in the burning rate law were based upon burning times obtained through closed chamber testing of the VHBR samples which were used for the traveling charge. Further, the ignition of the the traveling charge was delayed 1.15 ms after the ignition of the booster charge. The time delay used for the traveling charge was estimated from the experimental P/T curves. Table 3 summarizes the computed results and comparisons with the experimental data.

TABLE 3. Comparison of Predicted XKTC Results and Experimental Results for Traveling Charge Firing

Gage 1 Pmax (MPa)	Gage 2 Pmax (MPa)	Gage 3 Pmax (MPa)	Gage 5 Pmax (MPa)	Gage 7 Pmax (MPa)	Velocity Breakscreen (m/s)
XKTC -- Computed:					
554	472	620	89	39	1782
Experimental -- Traveling Charge (ID 12):					
555	458	590	98	44	1630
Difference:					
-1	14	30	-9	-5	152
Percent Difference:					
-.2%	3%	5%	-9%	-11%	8.5%

The P/T curves, both computed and experimental, are shown in Figure 4. As with the conventional case, XKTC results are in reasonable agreement with experimental results for breech pressure and timing. However, downbore pressures and velocity show a larger difference than for the conventional case.

Although pressure profiles for the breech gage are in close agreement, downbore pressure histories and velocity show a large deviation between experiment and computation. Possible explanations for this discrepancy involve bore resistance, blow-by, or incomplete TC combustion. It is likely that the bore resistance for the TC case was substantially larger than for a conventional firing. The TC propellant holder was 5 cm long and made of thin walled (0.04 cm) aluminum. The normal forces exerted by the TC burning can easily exceed 100 MPa which would, in an unconfined situation, rupture the holder. During a gun firing, the aluminum, instead of rupturing, may be forced out to the bore surface when the TC ignites creating a very large bore resistance. Consequently, calculations were carried out in which the bore resistance profile was increased. It was possible to decrease the calculated velocity for the traveling charge simulation from 1780 m/s to 1650 m/s by increasing the bore resistance from 20 MPa to 40 MPa. This brought the measured and calculated results into closer agreement. Evidence for a possible bore resistance increase is observed in Figure 5. Plotted in this figure is velocity versus time for the traveling charge firing, both calculated (constant bore resistance, 20 MPa) and experimental.

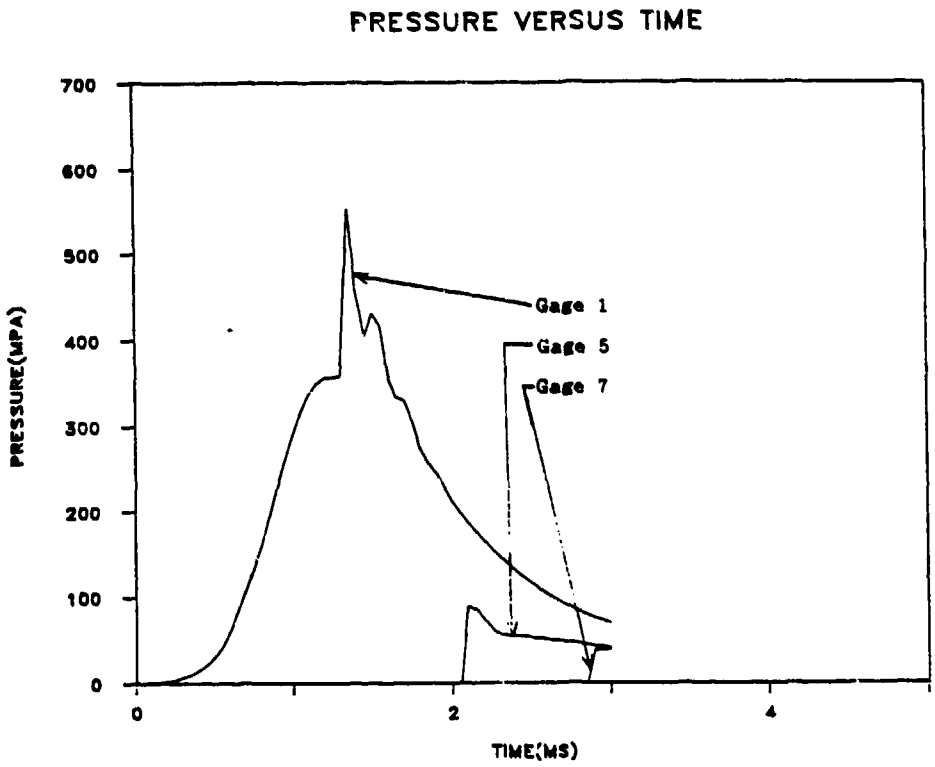

Figure 4a. Computed P/T Profiles for a Traveling Charge Gun Firing

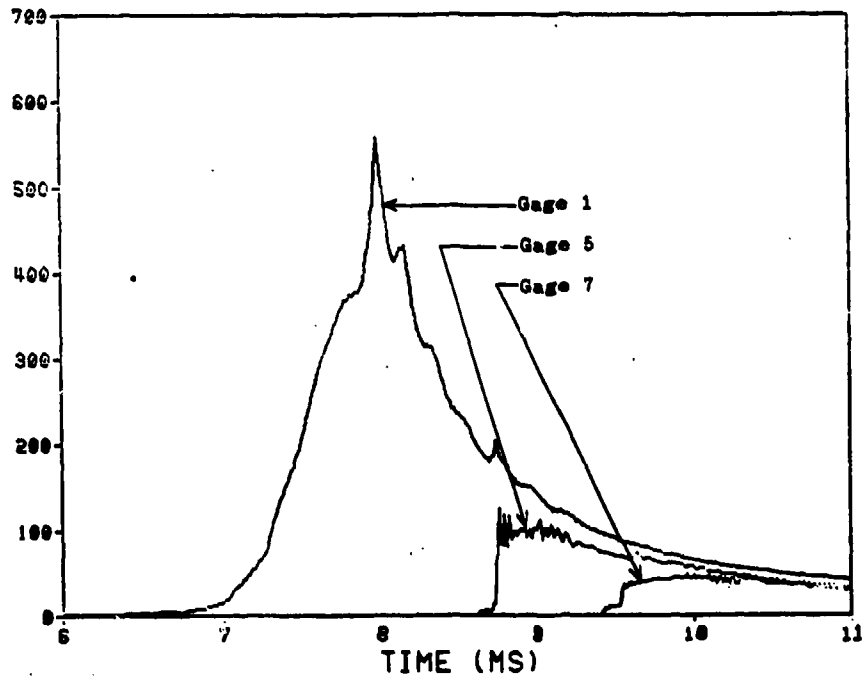

Figure 4b. Experimental P/T Profiles for a Traveling Charge Gun Firing

The curves are the same for the first part of the travel, up to A. The deviation from A to B may be due to increased bore resistance as described above. This higher resistance would result in both higher pressure and lower velocity. As mentioned earlier, lower experimental velocity may also be a result of gas blow-by. Referring to Figure 5, at B, the data from the interferometer was lost due to propellant gas blow-by, which has been verified by high speed films which show a large flash of light down bore at the same time that the interferometer signal is lost. The interferometer signal was recovered at C. Thus, substantial propellant gas blow-by (B to C) could result in a lowering of the velocity. The final explanation based on incomplete combustion of the traveling charge is discussed below.

To demonstrate the effect that the traveling charge can have on the interior ballistic process, consider the pressure and velocity histories for ID 44, a successful TC firing, and ID 49, (velocity only) where the TC did not ignite. These histories are given in Figures 6 and 7 Ignition of the TC is shown as point D in Figure 7. Prior to TC ignition, the pressures and velocities should be the same for both firings. Examination of the velocity histories (Figure 7) indicates that up until the time of maximum chamber pressure the velocities are

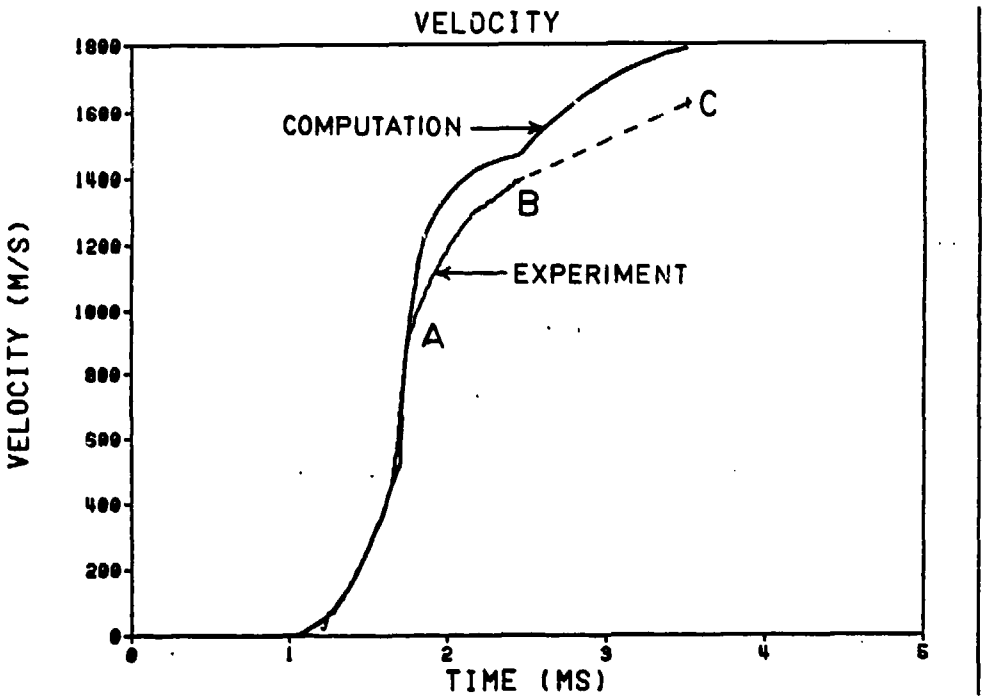

Figure 5. Comparison of Velocity for Computed and Experimental Results

identical. After this time the TC ignites (point D), and the acceleration is substantially increased for ID 44. Thus, ignition of the traveling charge results in improved acceleration and velocity without substantial increases in chamber pressure.

In simulating the traveling charge firings using XKTC the same input data that was utilized in simulating the conventional firings (booster propellant burn rate, as determined from closed chamber firings, and the resistance profile, as determined by matching calculated pressure and velocity histories with experiment) was used. Only characteristics of the traveling charge were varied to try to match calculations with experiment. An estimate of the TC ignition was made from an examination of the experimental velocity histories.

In the initial set of calculations previously discussed, a pressure-dependent burn rate law was used to describe the TC combustion. However, muzzle velocities were consistently larger than experimental velocities. Therefore, two changes, based upon experimental evidence, were made in the burning characteristics of the TC. First, since the calculated velocities were systematically high, it was speculated that not all of the 9.6 g of TC was burning and contributing energy to accelerating the projectile. There is some experimental evidence for this hypothesis. Closed chamber firings[9] have indicated that for this type of propellant the final pressures are not always identical with those predicted from thermochemical calculations. This could be due to incomplete combustion of the formulations. Also, a witness plate in

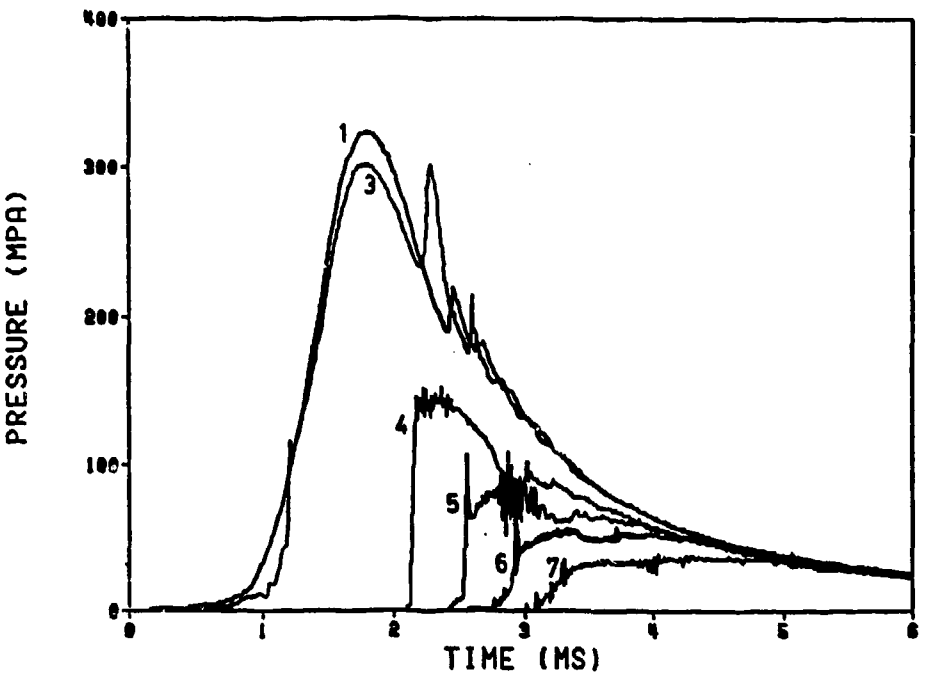

Figure 6. ID 44. Experimental Pressure
Late TC Ignition

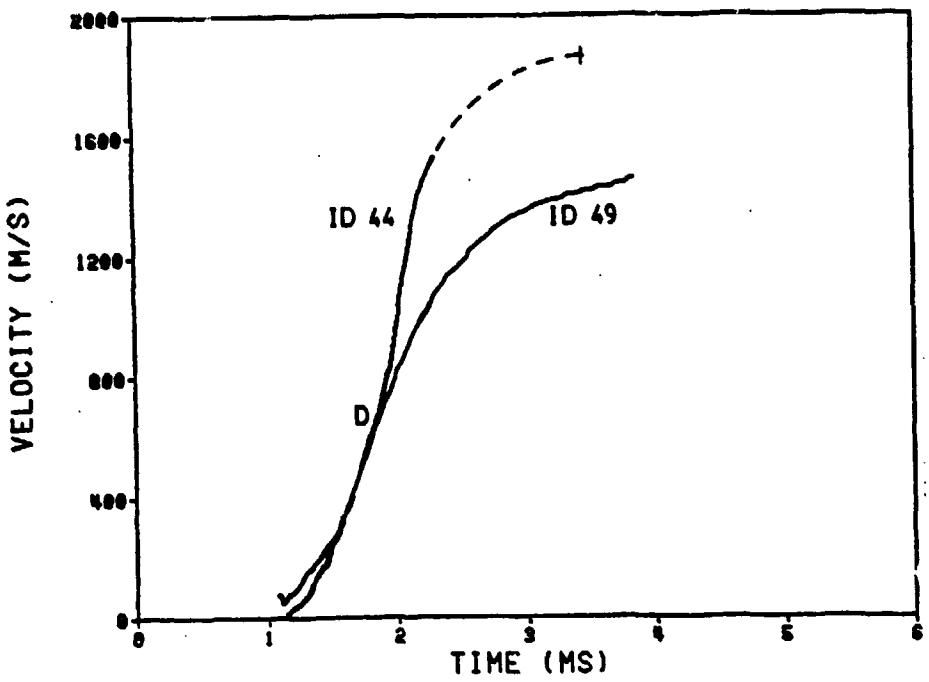

Figure 7. Experimental Velocity
(44) Late TC Ignition,
(49) No TC Ignition

front of the muzzle for the experimental firings has indicated that a substantial amount of small particulate matter is being accelerated with the projectile. This could be interpreted as unburned TC. Thus, a series of calculations was performed in which the burnt amount of TC, out of the total of 9.6 g, was varied. Second, closed chamber firings of a number of TC formulations have indicated that cylindrical samples, similar to those used in the traveling charge, burn with some form of deconsolidation rather than in a laminar fashion. Pressure histories indicate a decreasing mass generation rate as a function of burn time.[10]

As a consequence of these two observations, the TC combustion data used in the computations were altered in the following way. First, the total amount of TC burned was reduced from 9.6 g to 5.5 g, with the difference of 4.1 g being added to the projectile mass. Second, a dual burn rate law was introduced depending on the amount of TC burned,

$$r(m/s) = 127 \quad (0 \text{ to } 4.5 \text{ g})$$

$$r(m/s) = 25.4 \quad (4.5 \text{ to } 5.5 \text{ g}).$$

Thus, the first 4.5 g burned at the rate of 127 m/s and the final 1 g burned at a rate of 25.4 m/s.

Pressure and velocity histories for the simulation of ID 44 is shown in Figure 8 and 9. The agreement with the experimental results (ID 44, Figures 6 and 7) is reasonably good.

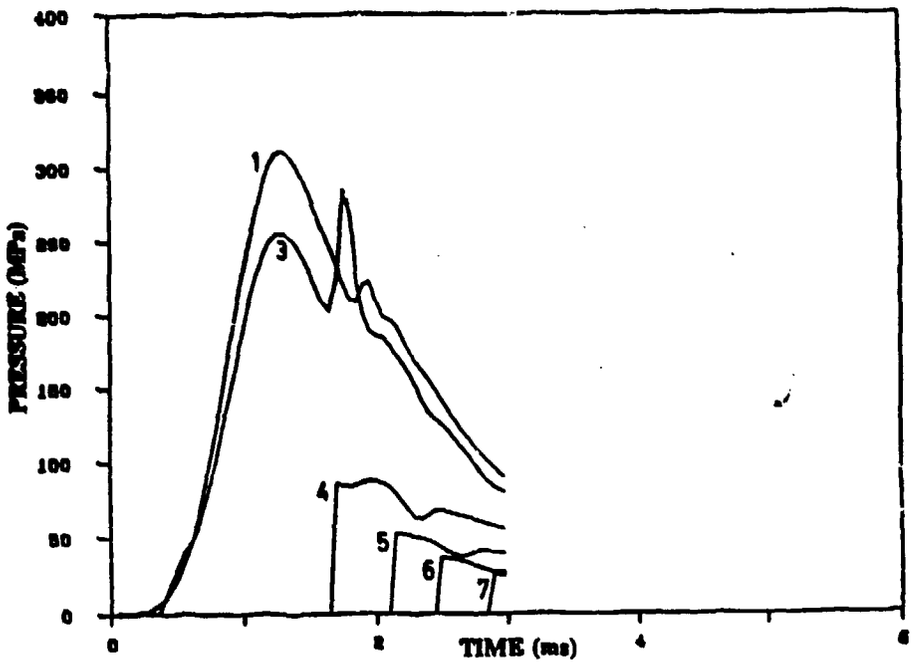

Figure 8. Simulation of ID 44 Pressure

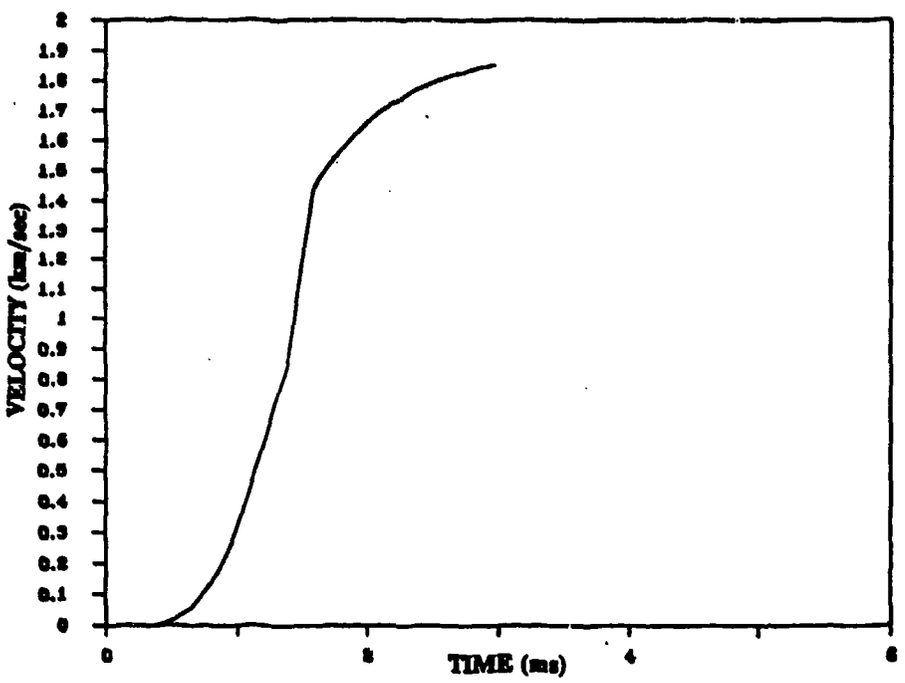

Figure 9. Simulation of ID 44 Velocity

III. PARAMETRIC INVESTIGATIONS

Since XKTC had demonstrated a reasonable predictive capability for both conventional and traveling charge gun firings in the small caliber gun system under study, a series of parametric calculations was performed to determine the effect of several factors which could impact traveling charge performance.

In order to maintain a set of realistic conditions which could be imposed on the gun system, ignoring uncertainties such as bore resistance, the following constraints were observed throughout the parametric study.

a) The web of the booster propellant was adjusted to produce a maximum gun pressure within 0.1% of 435 MPa.

b) The combustion characteristics of both the booster and the TC propellant were obtained from closed bomb combustion diagnostic observations. The burn rate law used to describe TC combustion was $r=bP^n$, with b=54.575 cm/(sec-MPa) and n=.95. These values for the burn rate law are equivalent to those used earlier in matching the TC firings. The exponent was reduced to .95 to increase stability of the numerical calculations in XKTC.

c) Propellant and projectile masses were those used, or could be used, in the 14-mm test fixture.

d) Except for the chamber geometry study, the gun dimensions used in the code were that of the BRL test fixture.

e) No bore resistance or shot start was used.

f) The velocity of TC combustion products, relative to the base of the TC, was not allowed to exceed Mach 1. This limitation is imposed by the equations used in the XKTC computer model.

1. CHAMBER GEOMETRY STUDY

The purpose of the chamber geometry study was to determine the effect that chamber length and the amount of chambrage could have on ballistic performance in the traveling charge context. Chambrage is defined, for the purpose of this report, to be the ratio of the diameter of the breech face, the rear of the chamber, to the diameter of the gun tube. The horizontal distance over which the coning due to the chambrage extends is referred to as the taper length. In the study, it was more convenient to work with the ratio of the taper length to the total chamber length than the amount of chambrage. In all instances, the total chamber volume was fixed at 100 cm^3. To maintain this fixed volume for various values of chambrage the breech face diameter was adjusted. To illustrate, consider Figure 10. In both the upper and lower diagram, total chamber length is 50.8 cm. For (a), the length of

the taper is 10.16 cm and the main chamber length is 40.64 cm; thus the length of the taper is 1/5 of the total chamber length. To maintain a volume of 100 cm^3, the breech face diameter is 1.577 cm. In (b), the taper length of 30.48 cm represents 3/5 of the total chamber length and requires a breech face diameter of 1.627 cm.

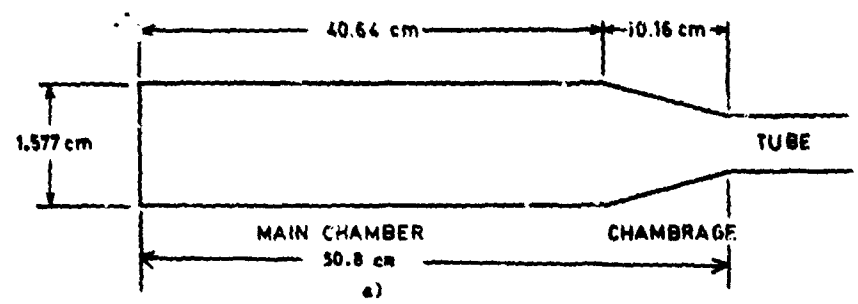

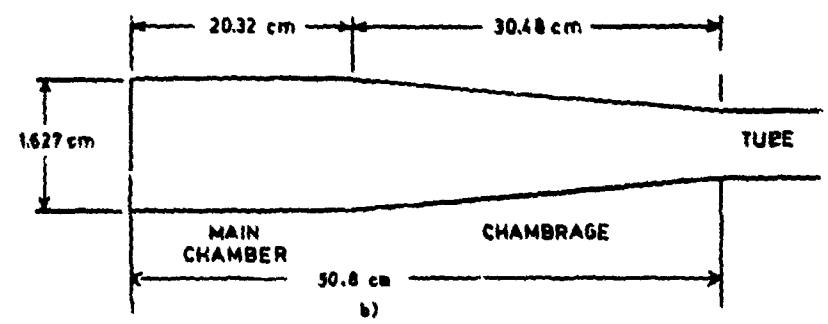

Figure 10. Varying Diameter for Differing Amounts of Chambrage

A bore diameter, 100 cm^3 chamber in the 14-mm gun is 63.5 cm in length. In the study, chamber lengths of 63.5, 50.8, 38.1, 25.4, and 12.7 cm with varying taper lengths were utilized. In all cases, 40 g of booster propellant, with burning characteristic identical to those of the non-deterred ball used in the experimental firings, was used. Propellant web was adjusted to obtain maximum gun pressures within 0.1% of 435 MPa. The mass of the TC was 8 g, and its ignition was delayed 0.5 ms after the attainment of maximum pressure from the burning of the booster propellant. Resulting velocities for the various configurations are presented in Table 4.

TABLE 4. Velocity (m/s) for Various Chamber and Taper Lengths

		CHAMBER LENGTH (CM)				
		63.5	50.8	38.1	25.4	12.7
	0/5	2206	****	****	****	****
	1/5	****	2247	2278	2287	2301
A T M A O P U E R R T	2/5	****	2246	2278	2285	2301
	3/5	****	2245	2278	2283	2300
	4/5	****	2248	2275	2288	2299
	5/5	****	2245	2272	2287	2301

Since a chamber length of 63.5 cm represents a bore diameter chamber, no chambrage is possible, hence the missing entries in column one of Table 4. Also, a shorter chamber having no taper length results in a chamber with a vertical rise at the tube entrance as shown in Figure 11. This type of sharp change in geometry represents a discontinuity, and the code would either not execute or produce results in which the energy or mass defects were large.

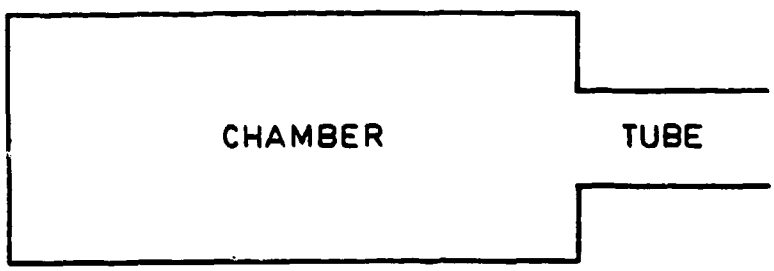

Figure 11. Discontinuity Resulting From Having No Taper Length

An examination of Table 4 indicates that the amount of chambrage or taper length appears to have little effect on muzzle velocity for a given chamber length, the maximum change being 7 m/s within any given column of the table However, there is a gain in velocity from the longest chamber, 63.5 cm, to a shorter chamber of 12.7 cm. The gain in velocity from the longest to the shortest length chamber is approximately 95 m/s, or a percent increase in velocity over the longer chamber of 4.3%. These observations are supported by an Analysis of Variance performed on Table 4. The results indicated no significant difference between rows but a significant difference between columns. A plot of velocity versus chamber length is shown in Figure 12. As can be

seen from the graph, the relation between velocity and chamber length is not linear, but more nearly a second order fit. Thus, a large portion of the benefit due to a shorter chamber can be obtained for a small percentage decrease in chamber length. For example, the gain in velocity in going from a chamber length of 63.5 cm to 38.1 cm is about 70 m/s of the total 95 m/s difference between the longest and shortest chamber length. This represents 74% of the total velocity increase, 70/95, for a 40% decrease in chamber length, 63.5 to 38.1 cm. The reasons for improved velocity performance with decreasing chamber length are addressed in a paper by Seigel.[11] To reiterate, these calculations were carried out for TC simulation. Similar results have also been observed for conventional gun simulations.[12]

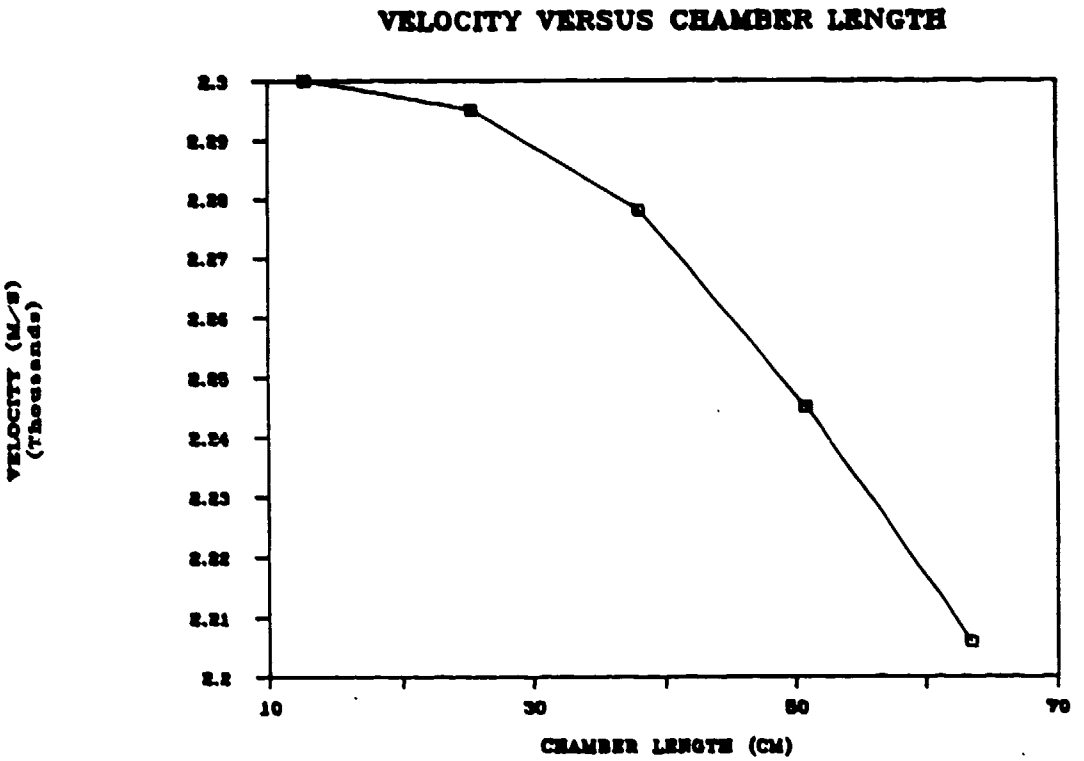

Figure 12. Velocity Versus Chamber Length

2. TC IGNITION TIME/LOCATION OF TC BURNOUT

TC ignition time refers to the time at which the TC ignites relative to the start of the ballistic event. For example, an ignition time of 1.15 ms means that the TC ignites 1.15 ms after the primer is ignited. Location of TC burnout refers to the position of the projectile in its travel at which the TC has totally burnt out. The two are considered together since a change in ignition time will affect the burnout position if the burn rate of the TC is held fixed. In the study, the gun geometry utilized in the code was identical to the 14-mm experimental gun fixture. Both booster and TC propellant burning

characteristics were taken from experimental results; however, booster mass and geometry were varied to obtain results for a variety of situations. TC mass in all cases was 8 g. As before, the web of the booster propellant was varied so as to maintain maximum gun pressure at 435 MPa. It should be pointed out that the maximum pressure of 435 MPa is due totally to the booster charge acting on the projectile and 8 g of traveling charge. If the burning of the TC caused pressures above 435 MPa, the web of the booster was not adjusted to reduce the pressure, and the simulation was not considered in the study. The purpose of the study was to determine if there was an optimal ignition delay for the TC to provide the maximum velocity and how sensitive was performance to variations in the TC ignition delay.

Typical results relating velocity to TC ignition time are presented in Table 5. For this case, 55 g of ball propellant was used as the booster propellant and projectile mass was 18 g. Maximum breech pressure occurred 1.63 ms into the event. TC ignition times prior to 1.63 ms result in gun pressures exceeding the 435 MPa constraint and were not considered as stated above.

TABLE 5. Velocity as a Function of TC Ignition Time

TC Ignition Time (ms)	Velocity (m/s)	
1.63	2256	
1.65	2260	
1.67	2264	
1.70	2274	
1.73	2280	
1.83	2306	
1.93	2332	
2.03	2355	
2.13	2375	
2.23	2400	
2.33	2417	
2.38	2424	
2.39	2421	TC did not burn out in bore
2.40	2415	
2.43	2396	
2.53	2332	
2.63	2272	
2.73	2211	

As can be seen from Table 5, as the TC ignition time increases up to 2.38 ms the velocity increases to 2424 m/s, an increase of 168 m/s (7.4%) over the velocity for TC ignition at 1.63 ms. For TC ignition times beyond 2.38 ms, the TC did not burn out in bore and the velocity decreases. Of importance for designing a practical traveling charge gun system is the sensitivity of velocity changes with TC ignition time. For instance, in this case the optimal TC ignition time is 2.38 ms. If

the TC ignition varies by 0.25 ms, velocity decreases significantly. For example, an ignition time of 2.13 ms produces a velocity of 2375 m/s, which is a drop of 49 m/s over the optimum 2424 m/s and represents a loss of 29% of the 168 m/s increase available from adjusting the ignition time. A delay of 0.25 ms shows an even greater loss. At an ignition time of 2.63 ms the velocity is down to 2272 m/s, which represents an almost total loss of the velocity gain from the ignition time of 1.63 ms to 2.38 ms.

Figure 13 summarizes the relation of velocity to TC ignition time for a variety of different propellant geometries and charge-to-mass ratios. No direct comparison between the velocities for the different cases should be made due to the different propellant and projectile masses used in the studies. However, the shape of the curve in each case is identical. Velocity increases with delayed ignition time up to a point. This point occurs at an ignition time beyond which all the TC does not burn out in the bore. <u>That is, for maximum performance the TC should burn out at muzzle exit.</u> For each curve, TC ignition times prior to those indicated on the graph result in breech pressure exceeding the 435 MPa constraint.

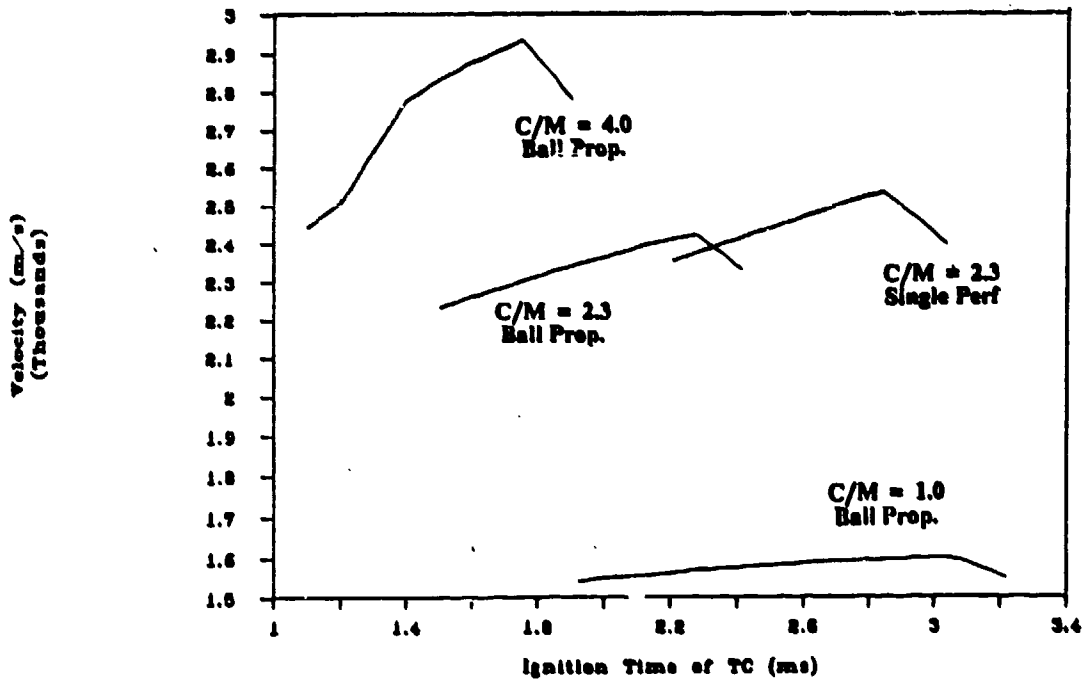

Figure 13. <u>Velocity Versus TC Ignition Time for a Variety of Simulations</u>

Also, the graphs of Figure 13 can be used to investigate the sensitivity of performance as a function of TC ignition time relative to different booster propellant geometries and charge-to-mass ratios. The slope of the graph, change in velocity divided by change in ignition

time, is a measure of this sensitivity. As can be seen in Figure 13, going from a c/m of 1 to a c/m of 4 for the ball propellant shows a large increase in slope. Although not shown, for larger c/m's the slope becomes even greater. However, the slope appears to be insensitive to changes in the type of booster propellant being used as long as the c/m remains constant as is illustrated for a ball and single perf propellant with a c/m of 2.3. Thus, the sensitivity of performance to changes in TC ignition time increases as the charge-to-mass ratio increases.

If the burning rate describing the combustion of the TC remains fixed, then changing the TC ignition time will change the location in the travel at which the TC burns out. Thus, investigating the effect of TC ignition time on performance also investigates the performance as a function of the location of the TC burnout. Figure 14 shows velocity versus the location of the TC burnout for the case presented earlier in Table 5. Total travel is 290 cm. It is clear from this graph that as TC burnout occurs closer to projectile muzzle exit, velocity increases. As expected, the location of burnout correlates directly to the TC ignition times listed in Table 5, with the last point of the graph corresponding to the TC ignition time of 2.38 ms.

As shown by Figures 13 and 14 and Table 5, tailoring the TC ignition time and the subsequent location of TC burnout can have a substantial effect, on the order of 7.4% for the case investigated, on the benefit to be derived through the use of traveling charge. It should be pointed out that the 7.4% represents only the change from the worst to best case traveling charge simulations and is not relative to corresponding conventional gun simulations which are detailed later in this report.

Clearly, not having TC burnout in bore should result in lowered velocities since additional energy must be expended to accelerate the parasitic mass, unburnt TC, attached to projectile. However, the reason for improved velocities with TC ignition times resulting in TC burnout near muzzle exit is not as obvious, since delaying TC ignition means that the unburnt TC must be accelerated farther down the tube. One possible explanation is presented in Figure 15. Shown are graphs of base pressure versus travel for two different traveling charge simulations with TC burnout at 135 cm (A) and 60 cm (O), respectively. For both of the graphs there are abrupt drops in pressure, from 200 to 100 MPa for curve O and from 100 to 50 MPa for curve A. The position in the travel at which the drop begins is approximately the location at which the TC burned out. Thus, burnout of TC in-bore appears to result in a drop in magnitude of about 50% in the base pressure. The cause for this drop is that TC burn-out results in a change in direction of combustion gas momentum from being directed toward the breach while the TC is burning to toward the muzzle after TC burnout. This abrupt change creates a strong rarefaction wave which appears as a large pressure drop. Since the energy imparted to the projectile is essentially the area under the base pressure versus travel curve, more energy will be delivered to the projectile by avoiding the large drop in base pressure. That is, a TC ignition time which results in TC burnout near muzzle exit will increase the energy delivered to the projectile.

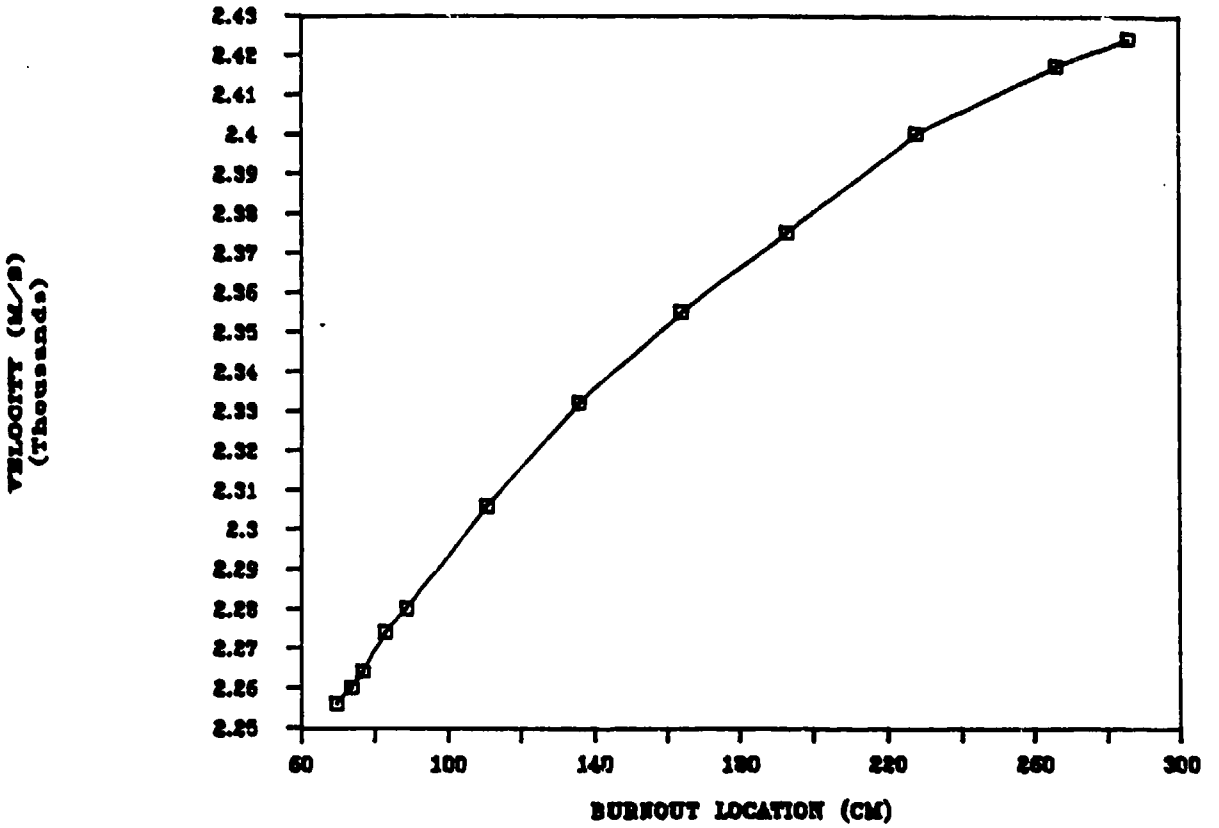

Figure 14. Velocity Versus Location of TC Burnout

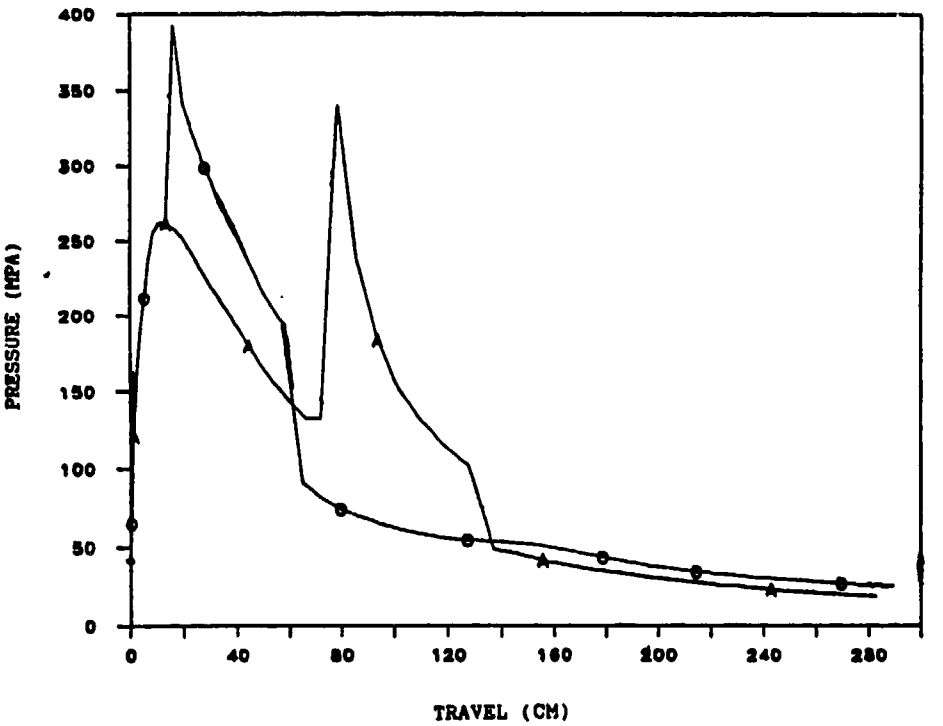

Figure 15. Base Pressure Versus Travel for Traveling Charge Simulations

3. TC PROPELLANT BURN RATE

The purpose of this part of the study was to investigate the effect that changing the TC burn rate would have on performance. In the study, the coefficient of the burn rate law, $r = bP^n$ with b=54.575 cm/(sec-MPa) and n=.95, used to describe the burning of the TC was changed to determine its effect on performance. The TC and booster masses were fixed at 8 and 55 grams, respectively. As in earlier studies, the web of the booster, a ball propellant, was adjusted to maintain the 435 MPa pressure constraint. Also, based upon the TC ignition time study, the ignition time of the TC was varied to obtain TC burnout at muzzle exit. Thus, in effect, the study investigated ballistic performance relative to the burning duration of the TC. Would a short rapid TC burn be more effective than a slower burn? Results of the study are summarized in Table 6. The maximum percent increase in the coefficient, over the baseline coefficient of 54.575 cm/(sec-MPa), was 80% to limit the Mach number of the TC combustion gases to less than unity.

As can be seen from the table, increasing the burn rate coefficient does result in increased velocity. However, the gain in velocity is rather small, only 54 m/s or a percent increase of 2.2% for the 80% increased coefficient case over the base case where the coefficient was 54.575 cm/(sec-MPa). Percent change in velocity as a function of percent change in burn rate coefficient for all the cases is shown in Figure 16. It is important to keep in mind that for the study the amount of TC was held fixed at 8 g. This is an amount that could be readily used in the 14-mm test fixture. However, if the TC had a higher burn rate, then more than 8 g could be used and burned out before muzzle exit. However, the potential benefit of a higher TC burning rate which would accrue from an increased mass of traveling charge to be used in the system was not addressed.

TABLE 6. Velocity Results for Changing Burn Rate Coefficient Describing the TC Combustion

% Change Coeff. (-)	Burn Rate Coeff. (cm./(sec-MPa))	Max. Mach Number (-)	Length of TC Burn (cm)	Velocity (m/s)
-10	49.118	0.527	172	2406
0	54.575	0.581	158	2424
+10	60.033	0.636	143	2434
+20	65.490	0.689	133	2447
+50	81.863	0.847	109	2466
+80	98.235	0.999	101	2478

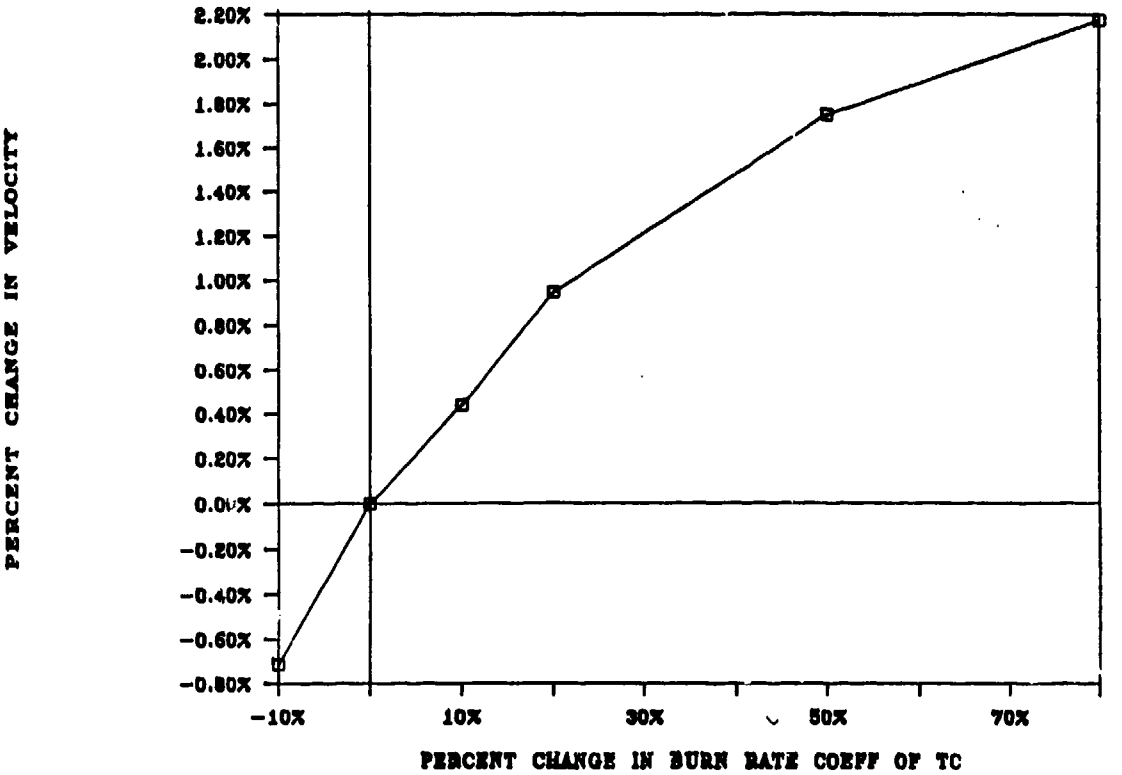

Figure 16. Percent Change in Velocity Versus Percent Change in the Burn Rate Coefficient Describing the TC Combustion

4. BOOSTER PROPELLANT GEOMETRY

It is generally accepted that for conventional gun systems the more progressive the grain geometry the better the resulting performance. For traveling charge gun systems it was felt that a more degressive geometry with the resulting earlier attainment of maximum pressure may be more beneficial. Thus, in this study three different grain geometries for the booster charge were investigated. The geometries were a ball which is a degressive geometry, a single perf with a large L/D which gives a neutral geometry, and a seven perf granulation which is a progressive geometry. First, the system, which was identical to the 14-mm test fixture, was optimized as a conventional gun system, by varying booster propellant mass and web to obtain the maximum velocity and stay within the constraint of a maximum breech pressure of 435 MPa for each of the three propellant geometries. In the optimization the mass of the projectile was 26 g. This mass for the projectile was selected to correspond to the normal 18 g projectile and 8 g of traveling charge propellant. Thus, the conventional optimization was to optimize the system for a traveling charge system up to the time at which the TC was ignited. Results of this optimization are given in Table 7. Unexpectedly, performance for the single perf granulation was almost 3% higher than that of the seven perf granulation. Similar results were obtained for a conventional (non-TC) larger caliber system using essentially the same charge-to-mass ratio.[13] At this time,

reasons for this result are not known. However, several theories involving propellant grain drag, grain slivering, and the high charge-to-mass ratio have been proposed and are under investigation.

TABLE 7. Optimization as a Conventional Gun System for Different Propellant Geometries, 26-g Projectile

Propellant Type (-)	Propellant Mass (g)	Velocity (m/s)
Ball	55	1936
1-Perf	63	2064
7-Perf	68	2008

The traveling charge was then introduced for the optimized conventional cases. Projectile mass was reduced to 18 g and the mass of the TC was 8 g. Again, due to the result of the TC ignition time study the ignition times for the TC were adjusted to optimize performance by having TC burnout close to muzzle exit. Results are given in Table 8. The inclusion of the traveling charge has resulted in increases of about 500 m/s in all three cases. Relative performance has remained the same with the single perf again outperforming the ball and seven perf propellant. Thus, for a fixed mass of TC, the propellant that optimized the system as a conventional gun also results in optimal performance when the traveling charge is allowed to burn.

TABLE 8. Velocity Corresponding to Various Booster Propellant Geometries in TC Gun Systems

Propellant Type (-)	Propellant Mass (g)	TC Mass (g)	Velocity (m/s)
Ball	55	8	2424
1-Perf	63	8	2534
7-Perf	68	8	2487

The belief that a more degressive propellant geometry would yield better performance was based on the fact that if the maximum pressure occurred earlier, then the traveling charge could be ignited at a earlier time. However, the TC ignition time study showed that the ignition time of the TC should be adjusted so that TC burnout occurs at muzzle exit. Thus, the results of Table 8 are not surprising, since for 8 g of TC the ignition is delayed well past the time of maximum pressure. A fairer test of the effect of different booster geometries would be to increase the mass of the TC to the maximum amount which

could be totally burnt before muzzle exit. This case was performed for the ball and the single perforated granulations. In addition, the burn rate coefficient of the TC was increased to 98.235 cm/(sec-MPa) which would allow for the most rapid burning of the TC without violating the Mach one limitation for TC combustion products. Results are shown in Table 9. As can be seen performance is virtually identical. All the benefit of using the more progressive, 1-perf, booster geometry has been overcome by the earlier attainment of maximum pressure of the ball propellant which allowed for a larger mass of TC to be burnt in-bore. Thus, it appears that the geometry of the booster charge does not play a critical role in ultimate traveling charge performance if the amount of TC is not fixed but allowed to be as much as can be burnt in tube.

TABLE 9. Optimal Velocity for Different Booster Propellant Geometries with the Maximum Amount of TC

Booster Propellant Type (-)	Booster Propellant Mass (g)	Traveling Charge Mass (g)	Projectile Mass (g)	Velocity (m/s)
Ball	55	34	18	2894
1-Perf.	63	29.75	18	2908

5. CHARGE-TO-MASS RATIO FOR 14-MM TEST FIXTURE

As was discussed earlier, the experimental firings to test the traveling charge concept were to be carried out in a 14-mm test fixture. There was an interest in knowing what were the optimum conditions for demonstrating the TC effect. For practical reasons, the initial tests would be done with approximately 8 g of TC. The question is, what is the best projectile weight to use to show the TC concept? Thus the objective was to determine if the benefit of the traveling charge was dependent on the overall propellant charge-to-projectile mass (c/m) ratio. A series of comparisons was made to examine the difference in velocity between conventional and traveling charge simulations as a function of c/m. In all cases a ball propellant was used for the booster charge, and the propellant diameter was varied to obtain a maximum gun pressure of 435 MPa. For the traveling charge simulations, 40 g of booster and 8 g of TC were used, and the charge mass was considered to be 48 grams for purposes of computing the charge-to-mass ratio. Again the ignition time of the TC was varied to force TC burnout just at muzzle exit. In the conventional calculations two different masses were utilized. In the first series of runs, 48 g of propellant was used so as to maintain constant energy for the comparison with TC. However, with 48 g of propellant, total burnout before projectile exit did not occur, and the propellant mass was lowered to 40 g resulting in total burnout and improved velocity. To obtain the desired charge-to-

mass ratio, the mass of the projectile was adjusted. Resulting velocities for the various configurations are presented in Table 10 and graphically in Figure 17.

TABLE 10. Velocity for Varying Charge-to-Mass Ratios in Conventional and Traveling Charge Simulations

C/M	Conventional			Conventional			Traveling Charge			
	Prop. Mass (g)	Proj. Mass (g)	Vel. (m/s)	Prop. Mass (g)	Proj. Mass (g)	Vel. (m/s)	Prop. Mass (g)	TC Mass (g)	Proj. Mass (g)	Vel. (m/s)
1/2	40	80	1185	48	96	1165	40	8	96	1177
1/1	40	40	1571	48	48	1543	40	8	48	1602
2/1	40	20	2012	48	24	1967	40	8	24	2109
3/1	40	13	2284	48	16	2220	40	8	16	2440
4/1	40	10	2479	48	12	2397	40	8	12	2681

As shown by Table 10 and Figure 17, as the c/m increases the benefits in increased velocity from using traveling charge improves. Table 11 summarizes the percentage increase in velocity resulting from using TC over the conventional case for the same charge-to-mass ratio. Thus the maximum increase in velocity for the 14-mm system occurs with the lightest weight projectile that is practical.

TABLE 11. Percentage Increases in Velocity Resulting from Using TC Over Conventional for Various Charge-to-Mass Ratios

C/M	Velocities			Percentage Increase of TC	
	TC (m/s)	Conv.(40g) (m/s)	Conv.(48g) (m/s)	Over 40 g Conv. (-)	Over 48 g Conv. (-)
1/2	1177	1185	1165	-0.7%	+1.0%
1/1	1602	1571	1543	+2.0%	+3.8%
2/1	2109	2012	1967	+4.8%	+7.2%
3/1	2440	2284	2220	+6.7%	+9.9%
4/1	2681	2479	2397	+8.1%	+11.8%

According to the theory of traveling charge as proposed by Langweiler,[1] the velocity gain of the projectile is obtained by transferring kinetic energy from the gas to projectile. Also, according to Corner[14] and Hunt,[15] as the charge-to-mass ratio increases the kinetic energy contained in the propelling gases increases. Thus, observing an increased benefit from traveling charge as the charge-to-mass ratio increases is to be expected from the traveling charge theory as long as the gas internal energy and energy loss remains constant. To

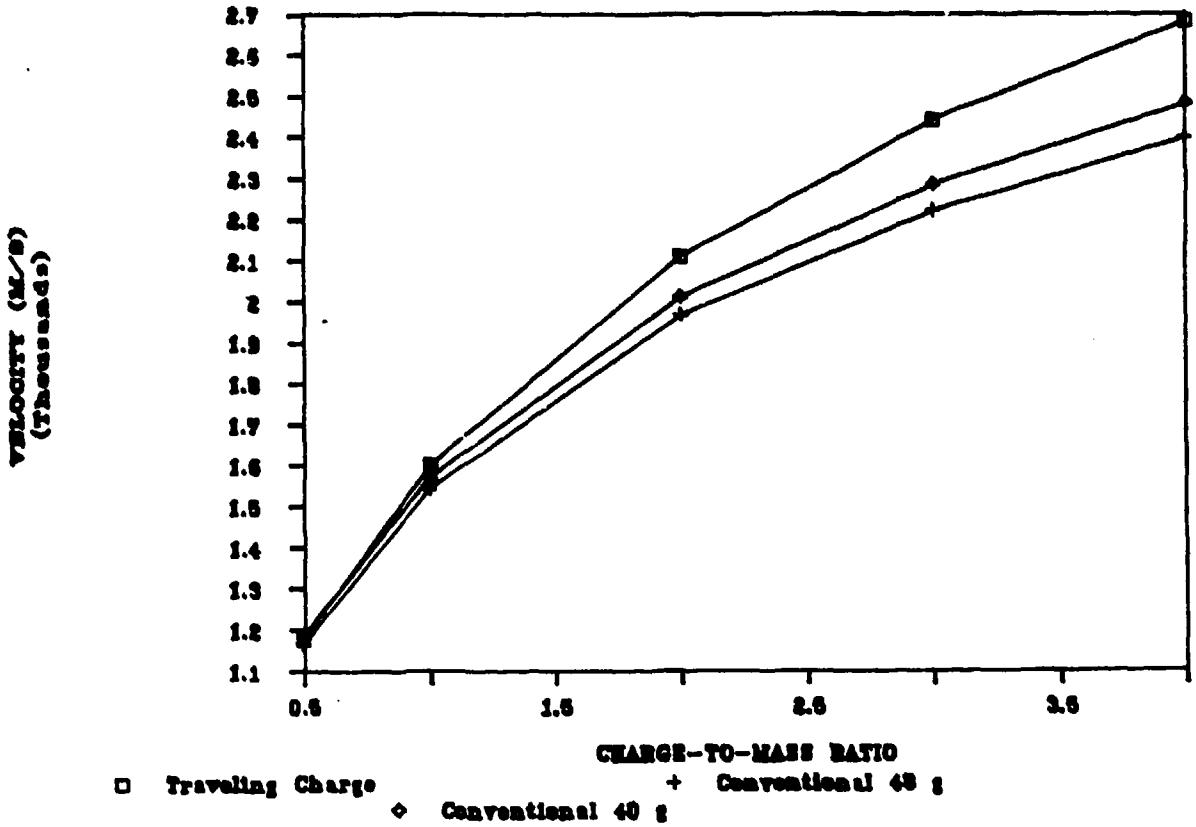

Figure 17. Comparison Between Conventional and Traveling Charge Velocities for Various Charge-to-Mass Ratios

determine if this indeed was the case for the simulations being performed, energy balances for the various runs, in terms of percentage of total energy available, were tabulated and are shown in Table 12. These calculations were carried out on the 14-mm system described in the previous section. The energies were determined at the time when the projectile was exiting the gun and is the sum of energy from the breech to the projectile base. The Energy Losses are the heat losses to the tube walls. The total KE is the sum of gas and projectile kinetic energies. As can be seen from the table, the sum of the gas internal energy and energy losses is roughly constant for each of the three basic propellant configurations, conventional 40 grams, conventional 48 grams, and traveling charge. Additionally, as the charge-to-mass ratio increases, the kinetic energy of the gas does increase, from about 5% to 16% of the total energy for conventional results and 2% to 11% for traveling charge. Therefore, in the traveling charge computations gas kinetic energy is reduced and the increase in kinetic energy or velocity of the projectile is obtained by decreasing the kinetic energy of the propellant gases as predicted by traveling charge theory.

TABLE 12. Energy Distribution from Conventional and Traveling Charge Calculations

C/M	Internal Gas Energy (%)	Energy Losses (%)	Gas Kinetic Energy (%)	Projectile Kinetic Energy (%)	Sum of Gas Internal and Losses (%)	Percent Gas KE is of total KE (%)
Conventional 48 g:						
1/2	49.6	19.7	5.0	25.7	69.3	16.3
1/1	51.4	18.0	8.1	22.5	69.4	26.5
2/1	53.3	16.3	12.1	18.3	69.6	39.8
3/1	54.6	15.3	14.5	15.6	69.9	48.2
4/1	55.5	14.8	16.1	13.6	70.3	54.2
Conventional 40 g:						
1/2	47.7	20.4	5.3	26.6	68.1	16.6
1/1	49.5	18.5	8.6	23.4	68.0	26.9
2/1	51.6	16.6	12.6	19.2	68.2	39.6
3/1	52.8	15.7	15.0	16.5	68.5	47.6
4/1	53.9	14.9	16.6	14.6	68.8	53.2
Traveling Charge - 40 g Booster, 8 g TC:						
1/2	53.6	18.0	2.1	26.3	71.6	7.5
1/1	54.6	16.7	4.4	24.3	71.3	17.5
2/1	55.9	15.4	7.6	21.1	71.3	26.4
3/1	57.6	13.9	9.6	18.9	71.5	33.7
4/1	57.8	14.0	11.2	17.0	71.8	39.7

IV. OPTIMAL PERFORMANCE FOR 14-MM BRL TEST FIXTURE

Having determined the importance of TC ignition time and burnout location, it was of interest to investigate the potential benefits which could be obtained through the use of the traveling charge concept. Thus, comparisons between optimal performance as a conventional gun versus the best traveling charge results, as predicted by XKTC, for the 14-mm gun fixture were determined (Table 13). The attempt here is simply to attain the maximum velocity possible from the system given a propellant type, with its mass and web allowed to vary, under a constraint of 435 MPa maximum gun pressure ("normal chamber"). In all computations no bore resistance was included since the actual bore resistance profile for the 14-mm test fixture is unknown. The "extended chamber" refers to enlarging the chamber to include the volume that would be occupied by the TC in the traveling charge simulation. Thus, the "extended chamber" cases are conventional simulations utilizing an increased chamber volume. The "fixed total energy" case refers to fixing the mass of propellant used in the conventional simulation to be

the same as the total mass used in the best TC simulation, in this instance 92.75 g (63 + 29.75), and then allowing the propellant web and chamber volume to vary to obtain optimal velocity. Finally, the "short tube" calculations refer to reducing projectile travel from 2900 mm, 200 calibers, to 1450 mm, a more realistic 100 calibers.

Several of the results from Table 13 are worthy of mention. First, the additional chamber volume resulting from the "extended chamber" has not resulted in an increase in velocity compared with the "normal chamber". Second, for the "normal chamber" the optimal results are obtained using a single perforated grain instead of the expected seven perf. Finally, "traveling charge simulation" predicts (2909 m/s) a velocity increase of 655 m/s, a 29% increase over the best conventional case (1-perf, "normal chamber", Table 13) and a velocity increase of 829 m/s, a 40% increase, over the "fixed energy" calculation. For the "short tube" configuration the calculations predict a 27.3% increase for traveling charge over conventional charge (2408 vs. 1891).

Table 13. XKTC Optimization of Experimental 14-mm Gun Fixture

Booster Type (-)	Booster Mass (g)	Traveling Charge Mass (g)	Projectile Mass (g)	Velocity (m/s)
NORMAL CHAMBER -- CONVENTIONAL FIRING				
Ball	53	-	18	2154
1-perf	58	-	18	2254
7-perf	60	-	18	2183
EXTENDED CHAMBER -- CONVENTIONAL FIRING				
1-perf	64	-	18	2239
7-perf	64	-	18	2182
FIXED TOTAL ENERGY(Optimal Loading Density)				
1-perf	92.75	-	18	2080
TRAVELING CHARGE SIMULATION				
1-perf	63	29.75	18	2909
SHORT TUBE				
1-perf	58	-	18	1891
1-perf	63	17	18	2408

V. CONCLUSIONS

Parametric studies with the computer code indicate that the traveling charge concept can offer substantially increased performance over conventional gun systems when hypervelocity performance is required. The implementation of the concept, however, requires a light projectile with a heavy propellant charge (a high c/m) and precise timing of both the ignition and burn out of the traveling charge propellant. Specifically,

1) Chamber geometry can have an effect on performance. Increases in velocity on the order of 4% can be obtained using a short chamber versus a longer chamber of the same volume.

2) The burn rate of the TC, per se, is not a critical factor; higher burn rates for a given amount of TC produce only a marginal increase in velocity (2.2% or less) over similar conventional guns. Burnout of the TC in-bore is crucial, however.

3) The optimal booster to use with TC appears to be the booster which optimizes the system as a conventional gun if a fixed amount of TC is used. If the mass of the TC is allowed to be as high as possible for optimal performance, then the booster propellant geometry appears to have little effect.

4) TC can yield substantial velocity increases (10% to 40%) over similar conventional guns depending on the overall propellant/projectile charge-to-mass ratio, with a higher overall charge-to-mass ratio favoring traveling charge.

5) The ignition time of the TC must be tailored to have TC burnout at muzzle exit. Performance drops off rapidly if burnout occurs before muzzle exit, or if all the TC does not burn out before muzzle exit.

The critical importance of the last factor cannot be over emphasized. The most significant technological hurdle to optimum TC performance remains the development of a precise ignition delay element.

REFERENCES

1. Langweiler, H., "A Proposal For Increasing the Performance of Weapons by the Correct Burning of Propellant," British Intelligence Objective Sub-Committee, Group 2, Ft. Halstead Exploiting Center, 1247.

2. Briand, R., Dervaux, M., Nicolas, M., "Etude Theorique De La Balistique Interieure De Canons Avec Charge Embarquee," AGARD Conference Proceedings No. 392, Interior Ballistics of Guns, AGARD-CP-392, January 1986.

3. May, I.W., Baron, A.F., Gough, P.S., Baer, P.G., "The Traveling Charge Effect," BRL Memorandum Report ARBRL-MR-03034, Ballistic Research Laboratories, Aberdeen Proving Ground, MD, July 1980.

4. Smith, H.C., "An Investigation of the Use of Porous Propellants in a Traveling Charge Gun," BRL Memorandum Report No. 1554, Ballistic Research Laboratories, Aberdeen Proving Ground, MD, January 1964. (AD#441254)

5. Tompkins, R.E., White, K.J., Oberle, W.F., and Juhasz, A.A., "Application of Very High Burning Rate Propellants to Traveling Charge," 24th JANNAF Combustion Meeting, Naval Postgraduate School, Monterey, CA, October 1987.

6. Gough, P.S., "The NOVA Code: A User's Manual. Volume 1. Description and Use," IHCR 80-8, Naval Ordnance Station, Indian Head, MD, December 1980.

7. Gough, P.S., "Extensions of BRLTC. A Code for the Digital Simulation of the Traveling Charge," Contract Report ARBRL-CR-00511, Aberdeen Proving Ground, Maryland, April 1983.

8. Oberle, W.F., White, K.J., Tompkins, R.E., and Juhasz, A.A., "Traveling Charge Computations - Experimental Comparisons and Sensitivity Studies," BRL-TR-2844, Ballistic Research Laboratory, Aberdeen Proving Ground, Maryland, August 1987.

9. May, I.W., Lynn, F.R., Juhasz, A.A., Fisher, E., Gough, P.S., "Thrust Characterization of Very High Burning Rate Propellants," ARBRL-MR-03359, Ballistic Research Laboratory, Aberdeen Proving Ground, MD, July 1984.

10. White, K.J., McCoy, D.G., Doali, J.O., Aungst, W.P., Bowman, R.E., Juhasz, A.A., "Closed Chamber Burning Characteristics of New VHBR Formulations," BRL-MR-3471, Ballistic Research Laboratory, Aberdeen Proving Ground, MD, October 1985.

11. Seigel, A.E., "Theory of High-Muzzle-Velocity Guns," Progress in Astronautics and Aeronautics, Volume 66, American Institute of Aeronautics and Astronautics, New York, New York, 1979.

12. Robbins, F.W., private communication.

13. Robbins, F.W., private communication.

14. Corner, J., "Theory of the Interior Ballistics of Guns," John Wiley & Sons, Inc., New York, New York, 1950.

15. Hunt, F.R.W., ed., "Interior Ballistics," The Philosophical Library, Inc., New York, New York, 1951.

DISTRIBUTION LIST

No. of Copies	Organization
12	Commander Defense Technical Info Center ATTN: DTIC-DDA Cameron Station Alexandria, VA 22304-6145
1	Commander USA Concepts Analysis Agency ATTN: D. Hardison 8120 Woodmont Avenue Bethesda, MD 20014
1	HQDA/DAMA-ZA Washington, DC 20310
1	HQDA, DAMA-CSM, E. Lippi Washington, DC 20310
1	HQDA, DAMA-ART-M Washington, DC 20310
1	HQDA/SARDA Washington, DC 20310
1	Commander US Army War College ATTN: Library-FF229 Carlisle Barracks, PA 17013
1	Director US Army BMD Advanced Technology Center PO Box 1500 Huntsville, AL 35807
1	Chairman DOD Explosives Safety Board Room 856-C Hoffman Bldg 1 2461 Eisenhower Avenue Alexandria, VA 22331

No. of Copies	Organization
1	Commander US Army Materiel Command ATTN: AMCPM-GCM-WF 5001 Eisenhower Avenue Alexandria, VA 22333
1	Commander US Army Materiel Command ATTN: AMCDRA-ST 5001 Eisenhower Avenue Alexandria, VA 22333-0001
5	Project Manager Cannon Artillery Weapons System, ARDEC, AMCCOM ATTN: AMCPM-CW, F. Menke AMCPM-CWW AMCPM-CWS, M. Fisette AMCPM-CWA, R. DeKleine H. Hassmann Picatinny Arsenal, NJ 07806-5000
2	Project Manager Munitions Production Base Modernization and Expansion ATTN: AMCPM-PBM, A. Siklosi AMCPM-PBM-E, L. Laibson Picatinny Arsenal, NJ 07806-5000
3	Project Manager Tank Main Armament System ATTN: AMCPM-TMA, K. Russell AMCPM-TMA-105 AMCPM-TMA-120 Picatinny Arsenal, NJ 07806-5000

DISTRIBUTION LIST

No. of Copies	Organization
1	Commander US Army Watervliet Arsenal ATTN: SARWV-RD, R. Thierry Watervliet, NY 12189
22	Commander Armament RD&E Center US Army AMCCOM ATTN: SMCAR-IMI-I SMCAR-TDC SMCAR-AE SMCAR-AEE-B, A. Beardell D. Downs S. Einstein S. Westley S. Bernstein N. Baron A. Bracuti J. Rutkowski L. Stiefel B. Brodman SMCAR-CCD, D. Spring SMCAR-AEE, J. Lannon SMCAR-AES, S. Kaplowitz SMCAR-CCS SMCAR-CCH-T, L. Rosendorr SMCAR-CCH-V, E. Fennell SMCAR-FSA-T, M. Salsbury Picatinny Arsenal, NJ 07806-5000
4	Commander US AMCCOM ATTN: SMCAR-ESP-L AMSMC-IRC, G. Cowan SMCAR-ESM(R), W. Fortune R. Zastrow Rock Island, IL 61299-7300
1	Director Benet Weapons Laboratory Armament R&D Center US Army AMCCOM ATTN: SMCAR-CCB-TL Watervliet, NY 12189
1	Commander US Army Aviation Research and Development Command ATTN: AMSAV-E 4300 Goodfellow Blvd St. Louis, MO 63120
1	Commander US Army TSARCOM 4300 Goodfellow Blvd St. Louis, MO 63120
1	Director US Army Air Mobility Research and Development Laboratory Ames Research Center Moffett Field, CA 94035
1	Commander US Army Communications Electronics Command ATTN: AMSEL-ED Fort Monmouth, NJ 07703
1	Commander ERADCOM Technical Library ATTN: STET-L Fort Monmouth, NJ 07703-5301

DISTRIBUTION LIST

No. of Copies	Organization
1	Commander US Army Harry Diamond Lab ATTN: DELHD-TA-L 2800 Powder Mill Road Adelphi, MD 20783
1	Commander US Army Missile Command Rsch, Dev, & Engr Ctr ATTN: AMSMI-RD Redstone Arsenal, AL 35898
1	Director US Army Missile & Space Intelligence Center ATTN: AIAMS-YDL Redstone Arsenal, AL 35898-5500
1	Commandant US Army Aviation School ATTN: Aviation Agency Fort Rucker, AL 36360
1	Commander US Army Tank Automotive Cmd ATTN: AMSTA-TSL Warren, MI 48397-5000
1	Commander US Army Tank Automotive Cmd ATTN: AMSTA-CG Warren, MI 48090
1	Project Manager Improved TOW Vehicle US Army Tank Automotive Cmd ATTN: AMCPM-ITV Warren, MI 48090
1	Program Manager M1 Abrams Tank System ATTN: AMCPM-GMC-SA, T. Dean Warren, MI 48090
1	Project Manager Fighting Vehicle Systems ATTN: AMCPM-FVS Warren, MI 48090
1	President USA Armor & Engineer Board ATTN: ATZK-AD-S Ft. Knox, KY 40121
1	Project Manager M-60 Tank Development ATTN: AMCPM-M60TD Warren, MI 48090
1	Director US Army TRADOC Systems Analysis Activity ATTN: ATAA-SL White Sands Missile Range, NM 88002
1	Commander USA Training & Doctrine Cmd ATTN: ATCD-MA/MAJ Williams Ft. Monroe, VA 23651
1	Commander USA Materials Technology Lab Dyna East Corporation ATTN: Christine P. Brandt, Document Control 3132 Market Street Philadelphia, PA 19104-2855
1	Commander US Army Research Office ATTN: Tech Library PO Box 12211 Research Triangle Park, NC 27709-2211

DISTRIBUTION LIST

No. of Copies	Organization
1	Commander US Army Belvoir R&D Ctr ATTN: STRBE-WC Tech Library (Vault) Bldg 315 Ft. Belvoir, VA 22060-5606
1	Commander US Army Logistics Ctr Defense Logistics Studies Ft. Lee, VA 23801
1	Commandant US Army Infantry School ATTN: ATSH-CD-CSO-OR Ft. Benning, GA 31905
1	President US Army Artillery Board Ft. Sill, OK 73503
1	Commandant US Army Command and General Staff College Ft. Leavenworth, KS 66027-5080
1	Commandant USA Special Warfare School ATTN: Rev & Tng Lit Div Ft. Bragg, NC 28307
1	Commander Radford Army Ammo Plant ATTN: SMCRA-QA/HI LIB Radford, VA 24141
1	Commander US Army Foreign Science & Technology Center ATTN: AMXST-MC-3 220 Seventh Street, NE Charlottesville, VA 22901

No. of Copies	Organization
1	Commandant US Army Field Artillery Center & School ATTN: ATSF-CO-MW, B. Willis Ft. Sill, OK 73503
1	Commander US Army Development and Employment Agency ATTN: MODE-TED-SAB Ft. Lewis, WA 98433
1	Office of Naval Research ATTN: Code 473, R.S. Miller 800 N. Quincy Street Arlington, VA 22217
2	Commander Naval Sea Systems Command ATTN: SEA 62R SEA 64 Washington, DC 20362-5101
1	Commander Naval Air Systems Command ATTN: AIR-954-Tech Lib Washington, DC 20360
1	Assistant Secretary of the Navy (R, E, and S) ATTN: R. Reichenbach Room 5E787 Pentagon Bldg Washington, DC 20350
1	Naval Research Lab Tech Library Washington, DC 20375
2	Commander US Naval Surface Weapons Ctr ATTN: J.P. Consaga C. Gotzmer Silver Spring, MD 20902-5000

DISTRIBUTION LIST

No. of Copies	Organization
3	Naval Surface Weapons Center ATTN: S. Jacobs/R10 Code 730 K. Kim/Code R-13 R. Bernecker/Code R-13 Silver Spring, MD 20902-5000
5	Commander Naval Surface Weapons Center ATTN: Code G33, J.L. East W. Burrell J. Johndrow Code G23, D. McClure Code DX-21 Tech Lib Dahlgren, VA 22448-5000
2	Commander Naval Underwater Systems Ctr Energy Conversion Dept ATTN: Code 5B331, R.S. Lazar Tech Library Newport, RI 02840
3	Commander Naval Weapons Center ATTN: Code 388, R.L. Derr C.F. Price T. Boggs Info Science Div China Lake, CA 93555-6001
1	Superintendent Naval Postgraduate School Dept of Mechanical Engr Code 1424 Library Monterey, CA 93943
1	Program Manager AFOSR Directorate of Aerospace Sciences ATTN: L.H. Caveny Bolling AFB, DC 20332
4	Commander Naval Ordnance Station ATTN: J. Birkett D. Brooks W. Vienne Tech Library Indian Head, MD 20640
1	HQ AFSC/SDOA Andrews AFB, MD 20334
1	AFRPL/DY, Stop 24 ATTN: J.N. Levine/DYCR Edwards AFB, CA 93523-5000
1	AFRPL/TSTL (Tech Library) Stop 24 Edwards AFB, CA 93523-5000
1	AFRPL/MKPB, Stop 24 ATTN: B. Goshgarian Edwards AFB, CA 93523-5000
1	AFFTC ATTN: SSD-Tech Lib Edwards AFB, CA 93523
1	AFATL/DLYV ATTN: George C. Crews Eglin AFB, FL 32542-5000
1	AFATL/DLJE Eglin AFB, FL 32542-5000
1	Air Force Armament Lab AFATL/DLODL Eglin AFB, FL 32542-5000
1	AFWL/SUL Kirtland AFB, NM 87117
1	Commandant USAFAS ATTN: STSF-TSM-CN Ft. Sill, OK 73503-5600

DISTRIBUTION LIST

No. of Copies	Organization
10	Central Intelligence Agency Office of Central Reference Dissemination Branch Room GE-47 HQS Washington, DC 20502
1	Central Intelligence Agency ATTN: Joseph E. Backofen HQ Room 5F22 Washington, DC 20505
1	General Applied Sciences Lab ATTN: J. Erdos Merrick & Stewart Avenues Westbury, NY 11590
1	Aerodyne Research, Inc. Bedford Research Park ATTN: V. Yousefian Bedford, MA 01730
1	Aeroject Solid Propulsion Co ATTN: P. Micheli Sacramento, CA 95813
1	Atlantic Research Corporation ATTN: M.K. King 5390 Cheorokee Avenue Alexandria, VA 22314
1	AVCO Everett Rsch Lab ATTN: D. Stickler 2385 Revere Beach Parkway Everett, MA 02149
1	Calspan Corporation ATTN: Tech Library PO Box 400 Buffalo, NY 14225
1	General Electric Company Armament Systems Dept ATTN: M.J. Bulman, R-1311 Lakeside Avenue Burlington, VT 05401

No. of Copies	Organization
1	IITRI ATTN: M.J. Klein 10W. 35th Street Chicago, Il 60616
1	Hercules Powder Co Allegany Ballistics Lab ATTN: R.B. Miller PO Box 210 Cumberland, MD 21501
1	Hercules, Inc Bacchus Works ATTN: K.P. McCarty PO Box 98 Magna, UT 84044
2	Director Lawrence Livermore National Laboratory ATTN: M.S. L-355, A. Buckingham PO Box 808 Livermore, CA 94550
1	Lawrence Livermore National Laboratory ATTN: M.S. L-355 M. Finger PO Box 808 Livermore, CA 94550
1	Olin Corporation Badger Army Ammunition Plant ATTN: R.J. Thiede Baraboo, WI 53913
1	Olin Corp/Smokeless Powder Operations R&D Library ATTN: V. McDonald PO Box 222 St. Marks, FL 32355

DISTRIBUTION LIST

No. of Copies	Organization
1	Paul Gough Associates, Inc. ATTN: P.S. Gough PO Box 1614 1048 South St. Portsmouth, NH 03801
1	Physics International Company ATTN: Library H. Wayne Wampler 2700 Merced Street San Leandro, CA 94577
2	Rockwell International Rocketdyne Division ATTN: BA08 J.E. Flanagan J. Gray 6633 Canoga Avenue Canoga Park, CA 91304
1	Princeton Combustion Rsch Lab ATTN: M. Summerfield 475 US Highway One Monmouth Junction, NJ 08852
1	Science Applications, Inc. ATTN: R.B. Edelman 23146 Cumorah Crest Woodland Hills, CA 91364
3	Thiokol Corporation Huntsville Division ATTN: D. Flanigan R. Glick Tech Library Huntsville, AL 35807
1	Scientific Rsch Assoc, Inc ATTN: H. McDonald PO Box 498 Glastonbury, CT 06033

No. of Copies	Organization
1	Thiokol Corporation Wasatch Division ATTN: Tech Library PO Box 524 Brigham City, UT 84302
2	Thiokol Corporation Elkton Division ATTN: R. Biddle Tech Library PO Box 241 Elkton, MD 21921
1	Universal Propulsion Company ATTN: H.J. McSpadden Black Canyon Stage 1 Box 1140 Phoenix, AZ 85029
2	United Technologies Chemical Systems Division ATTN: R. Brown Tech Library PO Box 358 Sunnyvale, CA 94086
1	Veritay Technology, Inc. 4845 Millersport Hwy PO Box 305 East Amherst, NY 14051-0305
1	Battelle Memorial Institute ATTN: Tech Library 505 King Avenue Columbus, OH 43201
1	Brigham Young University Dept of Chemical Engr ATTN: M. Beckstead Provo, UT 84601

DISTRIBUTION LIST

No. of Copies	Organization
1	California Institute of Tech 204 Karman Lab Main Stop 301-46 ATTN: F.E.C. Culick 1201 E. California Street Pasadena, CA 91109
1	California Institute of Tech Jet Propulsion Laboratory ATTN: L.D. Strand 4800 Oak Grove Drive Pasadena, CA 91103
1	Professor Herman Krier Dept of Mech/Indust Engr University of Illinois 144 MEB; 1206 N. Green St Urbana, IL 61801
1	University of Minnesota Dept of Mechanical Engr ATTN: E. Fletcher Minneapolis, MN 55455
1	Washington State University Dept of Mechanical Engr ATTN: C.T. Crowe Pullman, WA 99163
1	Case Western Reserve U. Division of Aerospace Sciences ATTN: J. Tien Cleveland, OH 44135
3	Georgia Institute of Tech School of Aerospace Engr ATTN: B.T. Zinn E. Price W.C. Strahle Atlanta, GA 30332
1	Institute of Gas Technology ATTN: D. Gidaspow 3424 S. State Street Chicago, IL 60616
1	Johns Hopkins University Applied Physics Laboratory Chemical Propulsion Information Agency ATTN: T. Christian Johns Hopkins Road Laurel, MD 20707
1	Massachusetts Institute of Technology Dept of Mechanical Engr ATTN: T. Toong 77 Massachusetts Avenue Cambridge, MA 02139
1	Pennsylvania State Univ. Dept of Mechanical Engr ATTN: K. Kuo University Park, PA 16802
1	University of Michigan Gas Dynamics Lab Aerospace Engr Bldg ATTN: Dr. G.M. Faeth Ann Harbor, MI 48109-2140
1	Purdue University School of Mechanical Engr ATTN: J.R. Osborn TSPC Chaffee Hall West Lafayette, IN 47906
1	SRI International Propulsion Sciences Division ATTN: Tech Library 333 Ravenswood Avenue Menlo Park, CA 94025

DISTRIBUTION LIST

No. of Copies	Organization
1	Rensselaer Polytechnic Inst. Department of Mathematics Troy, NY 12181
1	Director Los Alamos National Lab ATTN: M. Division, B. Craig T-3 MS B216 Los Alamos, NM 87545
1	Stevens Inst. of Tech Davidson Laboratory ATTN: R. McAlevy, III Castle Point Station Hoboken, NJ 07030
1	Rutgers University Dept of Mechanical and Aerospace Engr ATTN: S. Temkin University Heights Campus New Brunswick, NJ 08903
1	U. of Southern California Mechanical Engr Dept ATTN: OHE200, M. Gerstein Los Angeles, CA 90007
2	University of Utah Dept of Chemical Engineering ATTN: A. Baer G. Flandro Salt Lake City, UT 84112

Aberdeen Proving Ground

Dir, USAMSAA
ATTN: AMXSY-D
AMXSY-MP, H. Cohen

Cdr, USATECOM
ATTN: AMSTE-TO-F

No. of Copies	Organization
	Cdr, CRDEC, AMCCOM ATTN: SMCCR-RSP-A SMCCR-MU SMCCR-SPS-IL
	Cdr, USACSTA ATTN: S. Walton G. Rice D. Lacey C. Herud
	Dir, HEL ATTN: J. Weisz

USER EVALUATION SHEET/CHANGE OF ADDRESS

This Laboratory undertakes a continuing effort to improve the quality of the reports it publishes. Your comments/answers to the items/questions below will aid us in our efforts.

1. BRL Report Number_____ Date of Report_____

2. Date Report Received_____

3. Does this report satisfy a need? (Comment on purpose, related project, or other area of interest for which the report will be used.)_____

4. How specifically, is the report being used? (Information source, design data, procedure, source of ideas, etc.)_____

5. Has the information in this report led to any quantitative savings as far as man-hours or dollars saved, operating costs avoided or efficiencies achieved, etc? If so, please elaborate._____

6. General Comments. What do you think should be changed to improve future reports? (Indicate changes to organization, technical content, format, etc.)

CURRENT ADDRESS

Name

Organization

Address

City, State, Zip

7. If indicating a Change of Address or Address Correction, please provide the New or Correct Address in Block 6 above and the Old or Incorrect address below.

OLD ADDRESS

Name

Organization

Address

City, State, Zip

(Remove this sheet, fold as indicated, staple or tape closed, and mail.)